AN ABSTRACT OF THE THESIS OF

Diana R. Di Leonardo for the degree of Master of Science in Geology presented on November 28, 2012
Title: Regional Scale Sandbar Variability: Observations from the U.S. Pacific Northwest

Abstract approved:

Peter Ruggiero

Understanding sandbar dynamics and variability is integral to developing a predictive capacity for nearshore flows, sediment transport, morphological change, and ultimately for determining coastline exposure to damaging storm waves. Along the high-energy U.S. Pacific Northwest (PNW) coast, sandbars typically dominate the bathymetry of the active zone. Here we report on a nearshore bathymetric data set that covers an exceptionally long stretch of coast and crosses several littoral cell boundaries. Our study area stretches from Point Grenville, Washington to Cascade Head, Oregon, including 8 littoral cells and approximately 250 km in the alongshore. We describe and quantify the morphological variability of sandbars in the PNW over large spatial scales as well as attempt to explain the inter-littoral cell variability via trends and variability in environmental parameters. From 560 bathymetric profiles (~1000 km of measurements) we have extracted over 500 distinct subtidal sandbars. The bar zone extends to over 1km from the shoreline in the northern part of the study area, but only to about 600m in the southern part. Maximum bar crest depths are typically 7m below MLLW. Bar heights range from a step in the cross-shore profile to over 3m from crest to trough. The northernmost littoral cells typically have two or more bars per cross-shore profile whereas the littoral cells in the southern part of our study area have only one bar. The mean depths of the bars, however, are much more consistent across littoral cells. The mean depths remain consistent even while the upper shoreface slope significantly increases from north to south, requiring that the maximum bar distance from the shoreline decreases from north to south. This regional

gradient in upper shoreface slope is likely a response, at least in part, to a general coarsening trend in the sediment from north to south and hence linked to variations in regional geology.

©Copyright, by Diana R. Di Leonardo
November 28, 2012
All Rights Reserved

Regional Scale Sandbar Variability:
Observations from the U.S. Pacific Northwest
by
Diana R. Di Leonardo

A THESIS

submitted to

Oregon State University

in partial fulfillment of
the requirement for the
degree of

Master of Science

Presented November 28, 2012
Commencement June 2013

Master of Science thesis of Diana R. Di Leonardo presented on November 28, 2012

APPROVED:

____

Major Professor, representing Geology

____

Dean of the College of Earth, Ocean, and Atmospheric Sciences

____

Dean of the Graduate School

I understand that my thesis will become part of the permanent collection Oregon State University libraries. My signature below authorizes release of my thesis to any reader upon request.

____

Diana R. Di Leonardo, Author

ACKNOWLEDGEMENTS

Thank you to, my advisor, Peter Ruggiero for all your help and guidance. I have learned so much about coastal science and being a scientist from you. Thank you to my committee members, Rob Holman, Stephen Lancaster, and Gary Egbert, for your helpful feedback and time. Thanks to all the Nearshore All-stars and residents of the Coastal Imaging Lab, past and present, for your data collection efforts, your help and support, and lots of laughs along the way. You were an essential part of making my time at OSU enjoyable and productive. Thank you to all my fellow TA's for your moral support and advice; my students appreciate it, even if they don't know how much your support helped to keep me sane. Thanks to all the members of the Geomorphology Brown Bag for keeping the horizon of geomorphology broad for me. Thank you to my family and friends inside and outside of Corvallis for your support and understanding, even when I didn't call you back. Thanks to all the people who helped me along the way, but who I can't thank here because of the pages and pages it would require. I couldn't have done it without you.

Thanks to Deltares, The Northwest Association of Networked Ocean Observing Systems (NANOOS), the U.S. Army Corps of Engineers, and the Oregon Department of Geology and Mineral Industries (DOGAMI) for partially funding this work.

TABLE OF CONTENTS

Page

LIST OF FIGURES

LIST OF FIGURES (CONTINUED)

LIST OF TABLES

Regional Scale Sandbar Variability:
Observations from the U.S. Pacific Northwest

1 Introduction

Nearshore sandbars are found in the active zone of sandy coastlines worldwide, often contain substantial volumes of sand, and are important expressions of nearshore sediment transport. An understanding of their dynamics is important for coastal hazard and change prediction. Because these features can often dominate nearshore morphological variability, taking a large scale approach, by examining long duration and large-scale bathymetric data sets, can yield important insight into their characteristics and behavior (eg., Birkemeier, 1984; Lippmann et al., 1993; List and Terwindt, 1995; Grunnet and Hoekstra, 2004). Unfortunately, in-situ measurements of nearshore bars have historically been scarce due to the difficulty and expense of collecting such measurements. Few studies are continued over long time scales and even fewer encompass large spatial scales (Plant et al., 1999; Wijnberg, 2002; Ruessink et al., 2003; Grunnet and Hoekstra, 2004; Pape et al., 2010).

Given the difficulties of data collection, it is not surprising that large spatial and temporal scale sandbar variability is still poorly understood. Previous efforts have, in general, focused either on net offshore migration (NOM) or on classification systems for spatio-temporal variability. NOM has particularly intrigued the coastal community (Lippmann and Holman, 1990; Plant et al., 1999; Ruessink and Terwindt, 2000; Ruessink et al., 2003; Grunnet and Hoekstra, 2004; Ruessink et al., 2007; Pape et al., 2010; Kuriyama, 2012; Walstra et al., 2012; Wijnberg, 2002). Studies have described and characterized the cycle of bar generation near the shoreline, offshore migration, and bar degeneration well seaward of the shoreline (eg. Lippmann et al., 1993; Grunnet and Hoekstra, 2004) by identifying the timescales and patterns of NOM. Recent efforts have focused on modeling bar behavior (Ruessink et al., 2007; Pape et al., 2010; Kuriyama, 2012; Walstra et al., 2012). Predicting the onshore bar migration occurring between periods of offshore migration has proven to be the most challenging aspect of describing NOM. Larger scale studies have documented alongshore differences in the NOM behavior of bar systems along different coastlines and within longer stretches of coastline (Wijnberg and Terwindt, 1995; Wijnberg, 2002; Ruessink et al., 2003). Wijnberg (2002) correlated changes in temporal bar behavior over 120km of coastline with breaks in the shoreline, such as a jetty, and changes in offshore bathymetry, such as an ebb tidal delta, but truly satisfactory explanations of the underlying causes of differing bar behavior are still lacking.

Studies focused on spatial variability have used classification systems to characterize the longshore variability of sandbars (Wright and Short, 1984; Lippmann and Holman, 1990; van Enckevort and Ruessink, 2003a; Van Enckevort and Ruessink, 2003b;). Bar planforms, observed through video remote sensing of breaking patterns, are commonly classified as linear, rhythmic, or non-rhythmic. These efforts have primarily focused on the variability of a continuous outer or inner bar, over scales on the order of a kilometer (Lippmann and Holman, 1990; van Enckevort and Ruessink, 2003a; van Enckevort and Ruessink, 2003b), as a response to varying hydrodynamic conditions.

Here we report on approximately 250km of nearshore bathymetry data measured between 2010 and 2012 in the U.S. Pacific Northwest (PNW). Sandbars dominate the nearshore active zone of the PNW coast (Ruggiero et al., 2005), and this data provides an opportunity for characterizing the variability of sandbars at much larger spatial scales than has been previously attempted. The PNW region broadly shares the same geologic history and environmental forcing. Although the large-scale wave climate varies little at the regional scale, within the region there may be local alongshore variability in wave shoaling, refraction, and diffraction patterns over a heterogeneous bathymetry (García-Medina et al., in review). Likewise, local variations in the geologic and depositional history dictate the location of headlands and sand spits as well as the amount and type of sediment available on the beach. Here we investigate whether the alongshore variability of environmental forcing and underlying geology is expressed as differences in nearshore bar morphology at the regional scale.

The overall goal of this work is to describe and quantify sandbar morphological variability at the regional scale. More specifically, our objectives are to (1) quantify the spatial variation of sandbars over approximately 250km of the southwest Washington and northwest Oregon coastline, using observations from 2010-2012, (2) consider environmental variables that might cause or contribute to the variation observed in (1), and (3) put the observed spatial variability in the context of temporal bar variation. This work differs from the majority of previous studies because it examines morphological variability over extremely large space scales.

2 Study Area and Data Set

2.1 Study Area

The U.S. PNW is typically defined as the region spanning the states of Washington, Oregon, and northern California. This research focuses on a 262km long section of the PNW in southwest Washington and northwest Oregon. The southwest Washington coast is characterized by broad, low-lying accreted barrier beach plains (Peterson et al., 2010b; Vanderburgh et al., 2010) while much of the northern Oregon Coast is characterized by headlands separating pocket beaches. The largest Oregon headlands are highly effective at restricting sediment transport along the shoreline and delineate the Oregon littoral cells. Our study area encompasses 9 littoral cells (the four subcells of the Columbia River Littoral Cell, Cannon Beach, Rockaway, Netarts, Neskowin, and Sand Lake) (Figure 1). To maintain our focus on the regional scale, we concentrate on large, inter-littoral scale variability and trends.

The Columbia River Littoral Cell (CRLC) is the largest littoral cell in the study region and spans approximately 165 kilometers from Point Grenville, WA to Tillamook Head, OR. The CRLC is divided into the subcells of North Beach, Grayland Plains, Long Beach, and Clatsop Plains by large estuary mouths at the Columbia River, Willapa Bay, and Grays Harbor (Figure 1). All the subcells share the Columbia River as their sediment source; however because the Columbia River is not located at the center of the littoral cell, sediment delivery to each subcell does not occur at the same time and in the same amounts (Peterson et al., 2010b; Vanderburgh et al., 2010). Long Beach and Clatsop Plains receive the most direct sediment supply from the Columbia River and began prograding 4500 years ago (Peterson et al., 2010a). North Beach and Grayland Plains only receive sediment from the Columbia River after significant northward longshore transport and thus did not begin prograding until around 2800 years ago and 2500 years ago, respectively (Peterson et al., 2010a).

Five additional littoral cells are examined in northwest Oregon: Cannon Beach, Rockaway, Netarts, Neskowin, and Sand Lake (Figure 1). Within this section of the study region the littoral cells are delineated by headlands, which are much more common on the Oregon coast than in Washington. The estuaries are also much smaller than those in Washington. The Cannon Beach cell extends from Tillamook Head, Oregon to Cape Falcon, Oregon. Cannon Beach is characterized by a wide dissipative beach backed by coarse gravels and cliffs (Ruggiero et al., 2012). The Rockaway cell starts south of Cape Falcon and stretches 32km to Cape Mears. The coastline in Rockaway is interrupted by the entrances to Nehalem Bay and Tillamook Bay. The Netarts cell is the smallest littoral cell in our study area, and is located between Cape Mears and Cape Lookout. Netarts Spit (~9km long) is the dominant geomorphic feature of the littoral cell. The Sand Lake and Neskowin littoral cells are separated by Cape Kiwanda, a minor headland that is substantially smaller than either Cape Lookout to the north or Cascade Head to the south. We therefore combine these two small littoral cells (~15km) into a single analysis region (referred to hereafter as the Neskowin cell) as Cape Kiwanda projects seaward less than 0.5km from the shoreline and does not restrict sediment transport effectively. The Neskowin cell is defined as the coastline between Cape Lookout and Cascade Head.

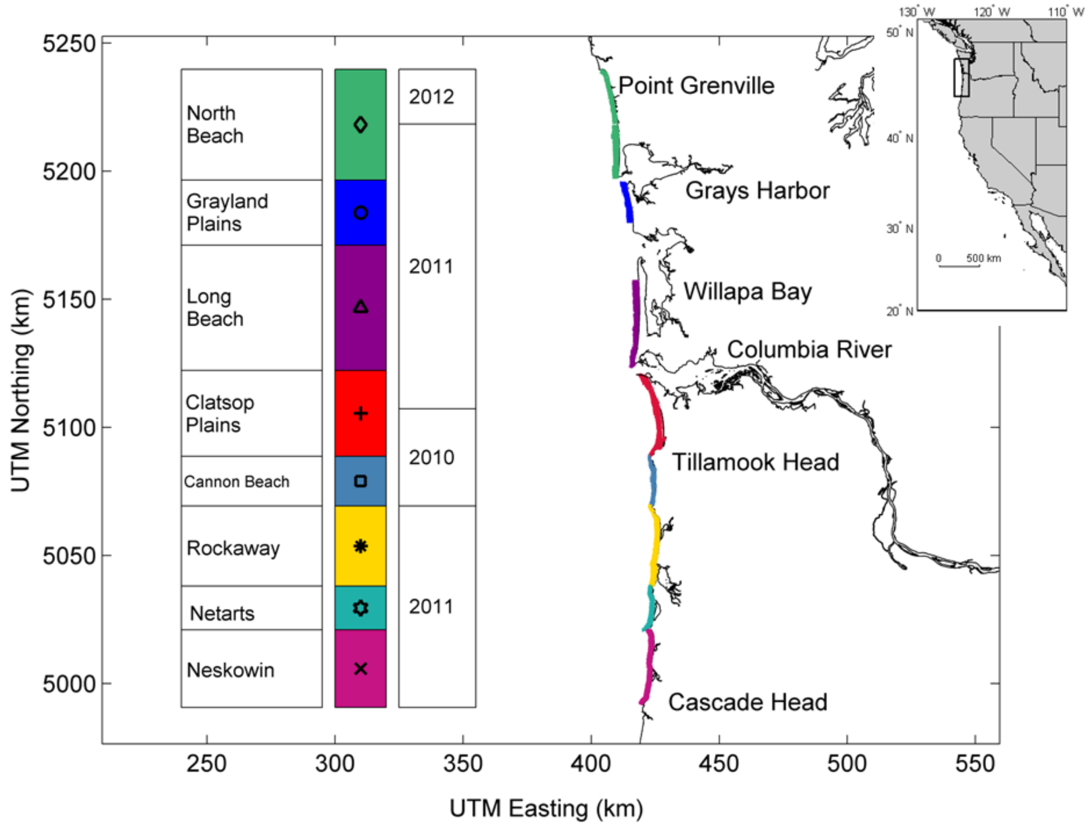

Figure 1. Map of study area showing broader continental context. The black box surrounds the study area on the continental map. Vertical bars show the year of data collection for each area, color and symbol assigned to each littoral cell, and name of each littoral cell. Areas of data collection are marked along the coast using the respective color of each cell.

The U.S. PNW experiences a highly energetic wave climate; winter storm significant wave heights reach 10m approximately once per year (Allan and Komar, 2002) and the average winter wave height for the study area is between 3m and 4m (Ruggiero et al., 2005). Average summer wave heights are between 1m and 2m. Mean wave direction also changes seasonally with winter waves approaching the coastline from a more southerly direction than summer waves (Ruggiero et al., 2005). Here we consider May through September as summer and October through April as winter, based on the frequency of storm events (Ruggiero et al., 2005).

Tides in the PNW are semidiurnal mixed and mesotidal. Mean tide ranges for the study area are between 2m and 4m (Komar, 1998). Although storm surge in the

PNW is relatively small (on the order of 1m), due to the narrow continental shelf, large winter storm waves combined with high tides regularly result in episodic erosion and flooding in the region (Ruggiero et al., 2001).

While sediment mixing from different sources in the PNW is presently limited, during lower stands of sea level sediments mixed throughout the region. During sea level transgression the sediments became isolated between headlands. North Beach, Grayland Plains, Long Beach, and Clatsop Plains are supplied with modern day sediment from the Columbia River (Clemens and Komar, 1988). South of Tillamook Head the mix of sediment mineralogies indicates multiple sources including the Umpqua River, the Klamath Mountains, and the Columbia River. The higher degree of rounding of these sediments, compared with present day Columbia River sediments, indicates that they are relict sediments emplaced before sea level transgression limited bypassing of the headlands (Clemens and Komar, 1988).

Sediments in the PNW overlie an erosional, geomorphic ravinement surface created by wave action during sea level transgression (Peterson et al., 2010; Vanderburgh et al., 2010). This surface slopes shallowly seaward (Vanderburgh et al., 2010); thus the upper shoreface slope is influenced not only by present day sediment characteristics, but also by the underlying geology. The modern slope is expected to be influenced both by the slope of the ravinement surface and by the thickness of the sediment fill above it, with the influence of the ravinement surface decreasing with increasing sediment thickness. Coring in the CRLC shows that the amount of wave erosion during the creation of the ravinement surface varied, and in places reached Pleistocene sediment (Vanderburgh et al., 2010). Approximately 5.5ka, erosion of the ravinement surface ceased near the Columbia River Mouth (Long Beach and Clatsop Plains), due to large inputs of sediment to the shoreline. Erosion continued in Grayland Plains for another thousand years, and active ravinement can still be found in North Beach in the form of recently eroded sea cliffs and a wave cut platform north of the Copalis River. The thickness of the Holocene sediment fill above the ravinement surface varies in the alongshore direction; approximate thicknesses are

30m in Clatsop Plains, 20m in Long Beach, 10m in Grayland Plains, and only a few meters in North Beach (Peterson et al., 2010; Vanderburgh et al., 2010). The ravinement surface is expected to exist throughout the PNW region, but has not been mapped south of Tillamook Head.

2.2 Data Set

In this study we utilize data from two separate beach monitoring programs in the PNW. Surveys of the CRLC began in 1998 as part of the Southwest Washington Coastal Erosion Study, a cooperative effort by the Washington Department of Ecology, the U.S. Geological Survey, and Oregon State University (Gelfenbaum and Kaminsky, 2010). Annual bathymetry and topography surveys in each of the CRLC littoral cells assess temporal beach evolution (Ruggiero et al., 2005; Ruggiero et al., 2007). More recently, similar nearshore bathymetric and topographic data has been collected in other areas of Oregon such as Reedsport, Clatsop County, and Tillamook County, through a partnership between Oregon State University and the Oregon Department of Geology and Mineral Industries (DOGAMI). These additional surveys allow us to analyze sandbar variability over a larger spatial extent but lack the multi-year temporal coverage of the CRLC data.

We utilize a nearshore bathymetric data set that covers 262km of the PNW coastline with 560 individual cross-shore profiles. In the cross-shore, the data set covers over 1000km. There is approximately 210km of sandy coastline in the study region. Only transects measuring the morphology along sandy coastlines were analyzed (465 transects) (Table 1). (For additional discussion of the transects that were analyzed see section 3.3 Bar Extraction.) The majority of the transects were surveyed in 2011 (>80%); however, in order to achieve continuous coverage of the region, we have included surveys from 2010 (15%) and 2012 (4%) (Table 1; Figure 1). The only gap in our coverage of the coastline in this region is ~ 3km north and ~11km south of Willapa Bay. The inlet to Willapa Bay is the largest natural channel in the study region. Not only is data collection in this area very hazardous, but the nearshore morphology is profoundly influenced by ebb tidal delta morphology and is not characteristic of the open coast dynamics that dominate in the rest of the study area.

Most bathymetric transects are accompanied by a complimentary topographic transect that aims to extend the profile continuously from approximately 2km offshore (~12 to 25m depth) through the surf zone to behind the foredune or to the base of coastal bluffs. Transects are spaced between 200m and 1km in the alongshore. The 1km spaced transects efficiently cover large sections of coast, while still effectively capturing the large-scale sandbar morphology; the 200m spacing captures greater detail of the morphology. Data collection at the regional scale requires some sacrifice of finer intra-littoral scale resolution for larger spatial coverage.

Four of the 8 littoral cells (North Beach, Grayland Plains, Long Beach, and Clatsop Plains) have been surveyed yearly since 1998 as part of the CRLC time series (Table 1) (Ruggiero et al., 2005; Ruggiero et al., 2007; Kaminsky et al., 2010;). We use the time series of bar morphology in the CRLC to address our third objective by placing the observed spatial variability in the context of interannual bar variation.

Table 1. Characteristics of the regional nearshore bathymetric data set. The amount of data for each littoral cell varies according to its length and the density of the transect spacing. Sandy coastline refers to the length of coastline not including headlands and estuaries.

Littoral Cell	Length of sandy coastline (km)	Total number of transects	Number of transects analyzed	Number of bars extracted	Years of data
North Beach	43	74	73	95	1998-2012
Grayland Plains	18	44	40	51	1998-2012
Long Beach	42	77	68	106	1998-2012
Clatsop Plains	29	90	65	82	1998-2012
Cannon Beach	15	47	36	60	2010
Rockaway	26	70	57	47	2008, 2009, 2011
Netarts	11	45	28	27	2011
Neskowin	26	113	98	84	2011
Total	**210**	**560**	**465**	**552**	**-**

3 Methods

Here we discuss the collection and processing of the profile data, the method of sandbar extraction, and the sources and resolution of the environmental variable data.

3.1 Data Collection

The nearshore bathymetry data used in this study was collected using a 4th generation coastal profiling system (CPS) (Beach et al., 1994; MacMahan, 2001; Ruggiero et al., 2007). The 4th generation system consists of a personal watercraft equipped with an onboard computer, monitor, RTK-DGPS, and a single beam echosounder (Ruggiero et al., 2007) (Figure 2). Earlier 'generations' of the CPS differ from the 4th generation in changes to equipment and boat configuration. CPS operators use Hypack® survey software to track their position with respect to a predefined (repeatable) transect. Experienced operators can maintain their position 'on line' to within about 2m and generally not more than 10m along the distance of a transect (Figure 3). Topographic surveys, walked with RTK-DGPS mounted on a backpack, accompany the bathymetric surveys to extend the profiles to the back of the foredunes or base of coastal bluffs (Figure 4). Operators are typically able to stay within 1m of their predefined survey line (Figure 3).

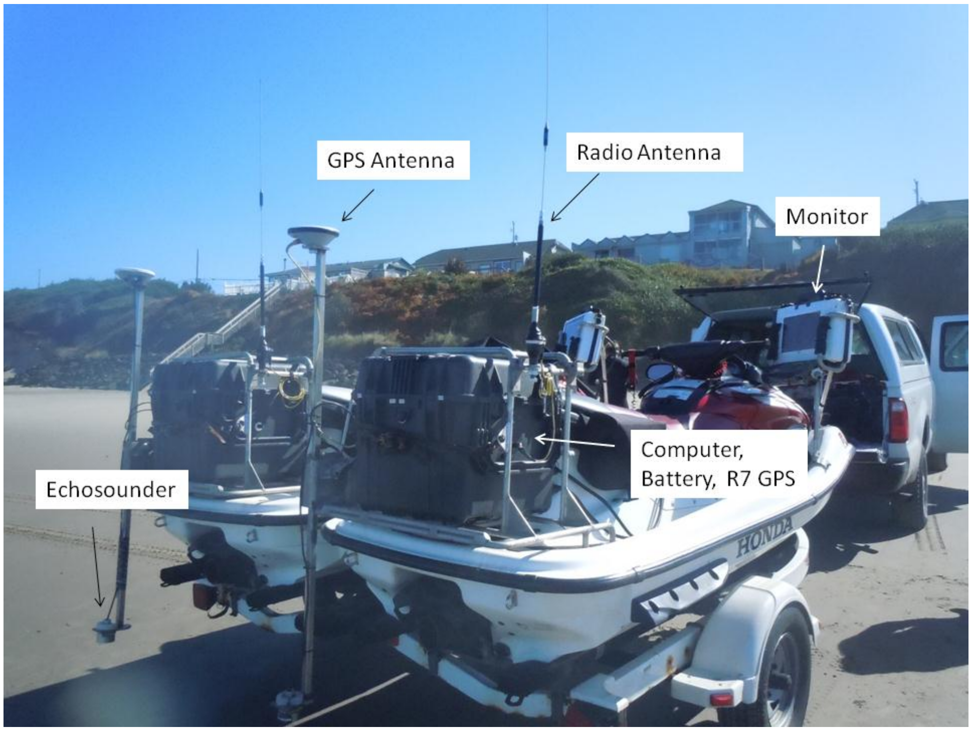

Figure 2. The CPS equipment set up for data collection includes a watertight case, monitor, echosounder, GPS and radio antennas. The case holds a small computer, the echosounder electronics, a Trimble R7 GPS unit, and a battery. Waterproof cables connect the equipment inside the case to the equipment mounted on the outside of the boat. The echosounder transducer and GPS antenna are rotated to a horizontal position during travel in shallow water to prevent the transducer from being damaged. The radio antenna allows the R7 rover unit to communicate with the base station. The monitor displays the transect, position and speed of the boat, and GPS status, enabling the CPS operator to maintain an 'on line' position as well as verify GPS and echosounder status during the survey.

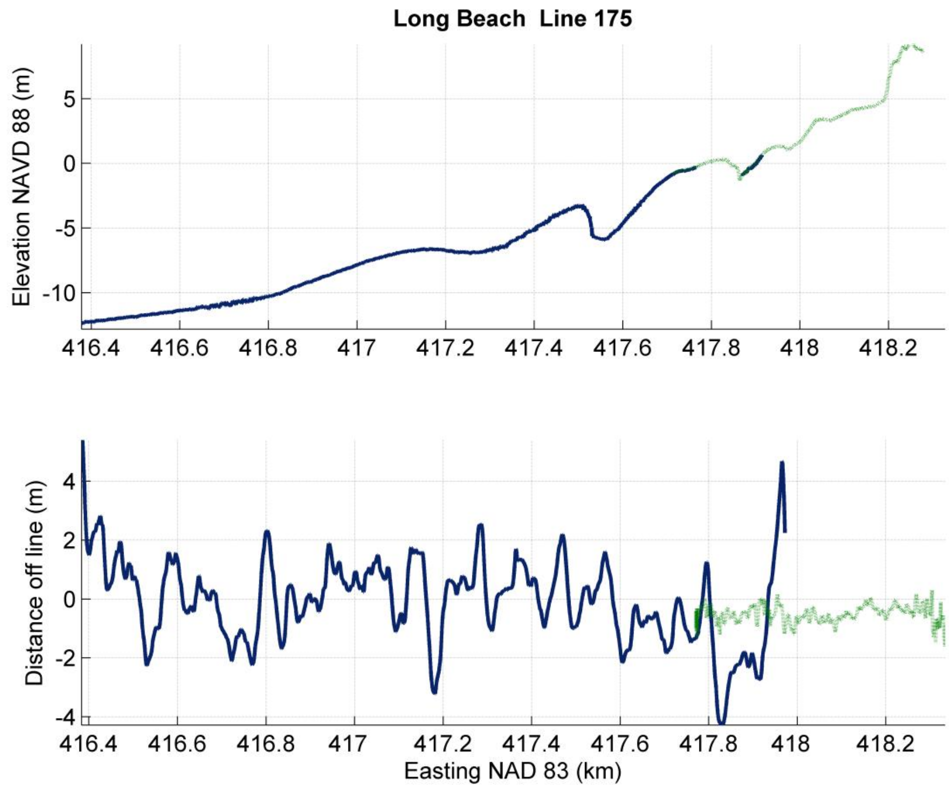

Figure 3. A merged bathymetry-topography profile extends from over 10m of water depth to the back of the dune. Top: An example transect with approximately 200m of overlap in the intertidal zone. Bottom: The ability of the operator to stay 'on line' during data collection differs for boat-based and land-based surveys.

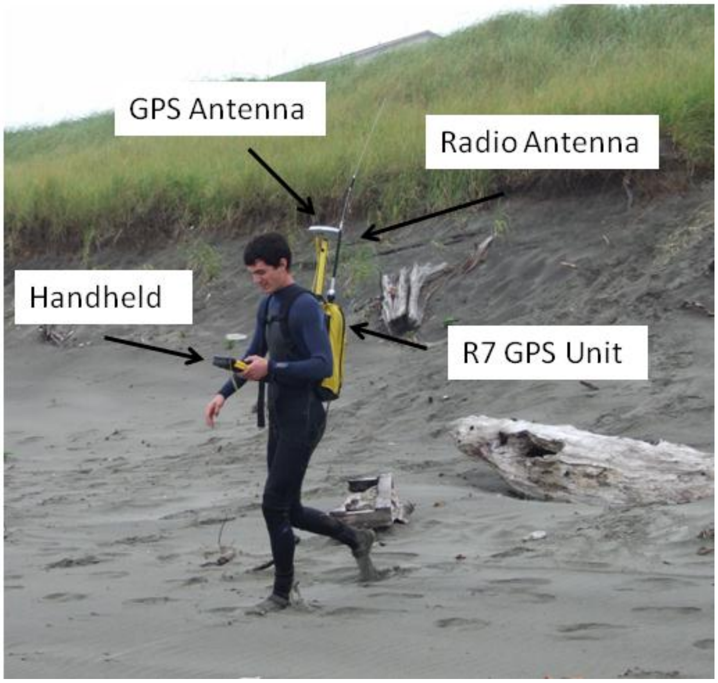

Figure 4. Topographic surveys use a handheld data logger to navigate while the GPS acquires position information. The radio antenna enables GPS communication with the base station. A measurement of the height of the GPS antenna for each operator is required to correctly record the elevation of the beach surface.

High levels of accuracy are possible with GPS surveys through the use of real time kinematic differential GPS (RTK-DGPS). To implement RTK-DGPS, a GPS base station is set up over a geodetic survey monument, the position of which is known to within centimeters (Daniels et al., 1999). Base stations are composed of a GPS antenna, GPS receiver, and a radio which is used to communicate position information to the rover units (CPS or backpack) (Figure 5). By communicating with the base station the rover units can locate their position relative to the survey monument to within centimeters. Manufacturer reported GPS errors are approximately 1cm in the horizontal and approximately 2cm in the vertical, with an additional 1cm of error for every 1km between the base station and the rover unit (Ruggiero et al., 2007). To further quantify the uncertainty of our measurements, we compare repeated survey lines between multiple survey boats and between survey days (Figure 6). Mean offsets between the repeat lines are consistently less than 10cm, and usually 5cm or less.

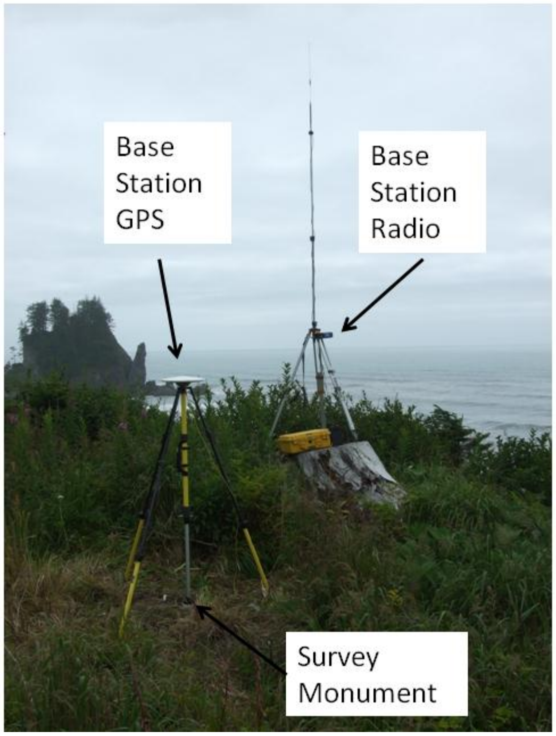

Figure 5. The base station is set up on a geodetic monument, the position of which is known to within centimeters. The radio transmits position information from the base station to the rovers improving positioning accuracy to centimeters. Rovers are typically within 10km of the base station.

While these repeatability tests and manufacturer reported errors suggest sub-decimeter accuracy, in practice, additional errors are introduced into the measurements. GPS drift caused by satellite geometry, satellite obstructions, and atmospheric conditions can be up to 10cm (Sallenger et al., 2003). Local site calibrations are performed for the topography surveys to reduce these errors to 4cm by occupying 2-5 geodetic monuments with the survey equipment and using a 3 parameter least squares fit to fix all data points within the survey network. Repeat topography surveys of a single line in a single day suggest additional repeatability errors of 4cm (Ruggiero and Voigt, 2000). Typical baseline distances of 5km yield a GPS error of 6cm. Combining the calibration error (~4cm), repeatability error (~4cm), and GPS error (~6cm) in quadrature yields a total error of 0.08m for the topography surveys (Ruggiero et al., 2007).

The bathymetry surveys suffer from the same GPS induced errors described above. In addition, water temperature variability can also lead to significant differences between the speed of sound at the time of the survey and the speed of sound employed by the echosounder in the depth calculation (typically 1500 m/s). In 12m of water, a 10°C variation in temperature can lead to up to 20cm of variation in estimates of the bottom depth (MacMahan, 2001). However, because water temperature in the PNW varies relatively little, this typically does not introduce additional significant errors into the measurements (Ruggiero et al., 2007). Adding the GPS drift error (up to10cm), the manufacturer reported GPS errors (~6cm), and the repeatability error (up to 10cm) in quadrature yields a conservative estimate of 0.15cm for vertical measurement error (Ruggiero et al., 2007). It is possible to resolve the bathymetry precisely despite the influence of tides and waves because the GPS and echosounder sample at a high rate; on the 4th generation CPS, the GPS samples at 20Hz and the echosounder samples at a maximum of 20Hz, depending on water depth and boat speed. All surveys are referenced to the North American Datum of 1983 (NAD 83) in the horizontal and to the North American Vertical Datum of 1988 (NAVD 88) in the vertical.

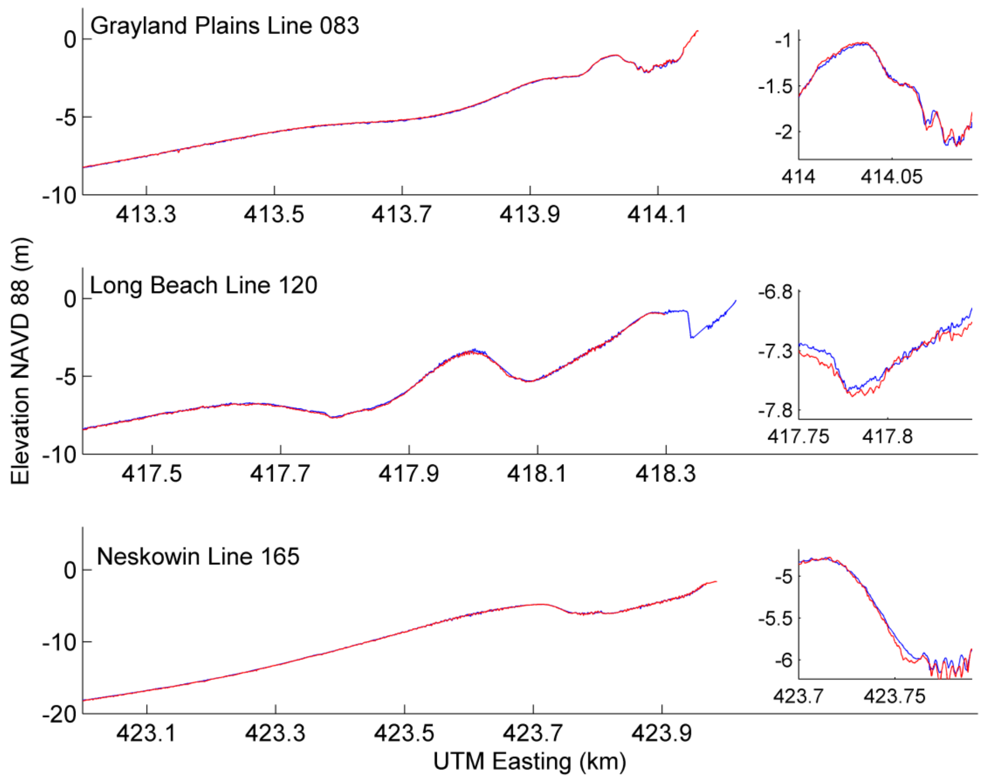

Figure 6. Repeatability tests show that multiple sets of bathymetry data from one line, surveyed by different boats, on the same day have sub-decimeter offsets. Blue line: Boat 1. Red line: Boat 2. The mean offset of each pair of profiles is 2cm, 4cm, and 5cm, from top to bottom, respectively. Insets show finer scale detail of the repeat profiles. Conditions during these surveys consisted of approximately 1.5 m significant wave heights and 7 second average wave periods as given by local wave buoys. The two lines from Long Beach were surveyed on consecutive days.

3.2 Data Processing

The raw echosounder returns are initially digitized by the internal signal processing algorithm of the echosounder, and then post-processed after the survey with two goals in mind: (1) eliminate digitization gaps, and (2) mitigate the effects of boat pitch and roll. Digitization gaps can be eliminated by viewing the raw echosounder full waveform returns, upon which the initial digitized profile is based, and adjusting the variables the algorithm uses for data recognition or by manually digitizing the raw returns. The effects of boat pitch and roll are reduced by identifying and removing sharp changes in the depth soundings. Along sandy coasts changes in the bathymetry are relatively smooth, and sharp changes in the bottom can be attributed to boat motion. Along rocky coastal areas sharp changes in the bathymetry are often real morphological features; data processing in these areas is more difficult and requires careful consideration of the raw echosounder returns. The final step in data processing is a minor smoothing operation using a combination of a standard deviation filter and a running average filter. For the standard deviation filter, the data are split into groups of approximately 10 points. Then outliers that are more than 1.5 standard deviations from the mean within each group of points are removed. The running average filter then smoothes the remaining data over groups of 5-10 points (typically 1m or less). Linear interpolation fills short (<25m) gaps. Processing is accomplished using a custom Matlab Graphical User Interface (GUI) (Andrew Stevens, USGS, personal communication).

3.3 Bar Extraction

In order to systematically quantify nearshore morphological variability, it is necessary to define specific features of the sandbar that can be reliably, consistently, and automatically extracted. We use three morphometric parameters to characterize the morphology: bar crest position from the shoreline, bar crest depth, and bar height (Figure 7). The distance from the shoreline is defined as the along-transect distance from the 2.1m contour to the bar crest. This shoreline elevation is referenced to NAVD88, and is based on a LiDAR derived operational mean high water (MHW) datum originally developed by the USGS (Weber et al., 2005). For transects with a corresponding topography survey, the 2.1m contour is extracted from the topographic data. The location and density of most of the Oregon transects was chosen based on the location of infrastructure and population density. Because these surveys were designed with different goals in mind than the CRLC surveys, for some of the Oregon transects there is no topography transect that directly corresponds to the bathymetry transect. In these instances, the surrounding topography surveys are used to interpolate the position of the shoreline (Figure 8).

The bar depth is defined as the depth below 0m NAVD88, which is typically within a decimeter of mean lower low water (MLLW). Bar height is defined as the difference between the depths of the bar crest and bar trough (Figure 7).

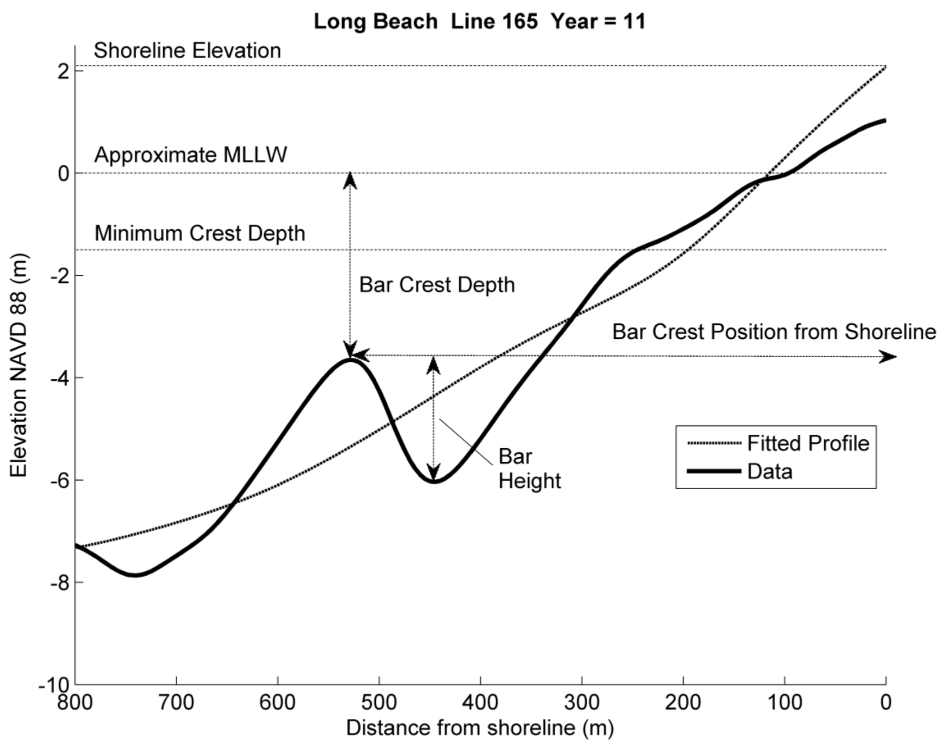

Figure 7. Definition sketch of sandbar morphometric parameters. Coverage of the intertidal zone is often incomplete; therefore intertidal bars (shallower than -1.5m) are not considered in subsequent analysis.

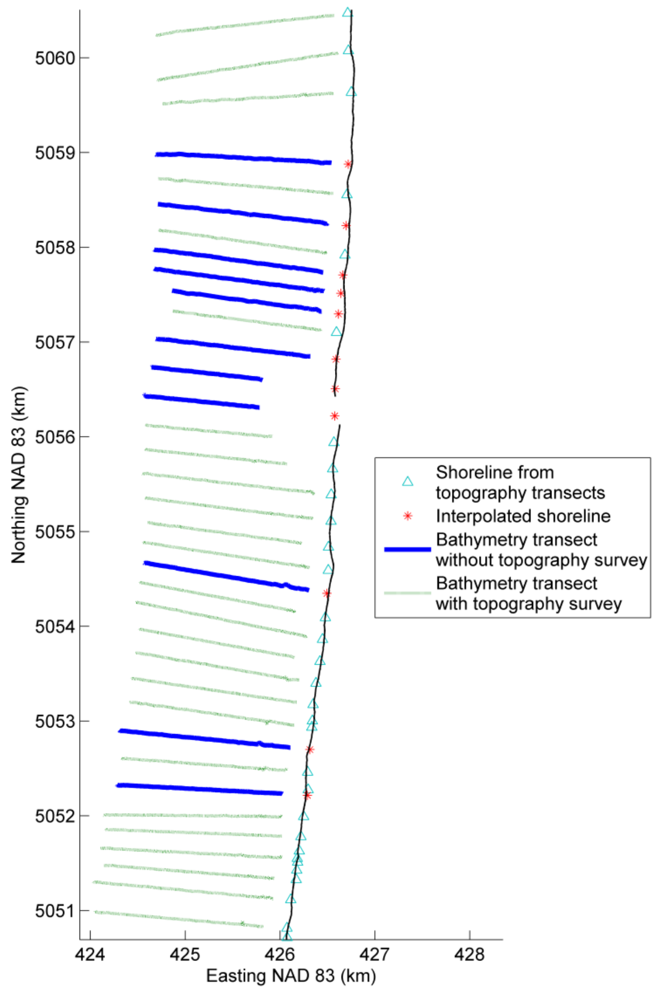

Figure 8. Bathymetry transects without corresponding topography transects have an interpolated shoreline based on the surrounding topography transects. The position of the interpolated shorelines is consistent with the position of the shoreline located on topography transects.

An established method for extracting sandbar morphometrics is by subtracting the mean profile over many years from the profile of interest to obtain a perturbation profile (Ruessink and Kroon, 1994; Plant et al., 1999; Grunnet and Hoekstra, 2004). Mean profiles in the CRLC do not entirely eliminate bar-like features (Figure 9), therefore in order to use the mean profile to recognize sandbar perturbations, we must first eliminate these features. We further smooth the mean profile with a loess smoother to remove features with a wavelength of less than 500m (Figure 9) (Plant et al., 2002). The extra smoothing step effectively removes the residual bar-like features (seen in blue) to create the bar-less profile (seen in black) (Figure 9).

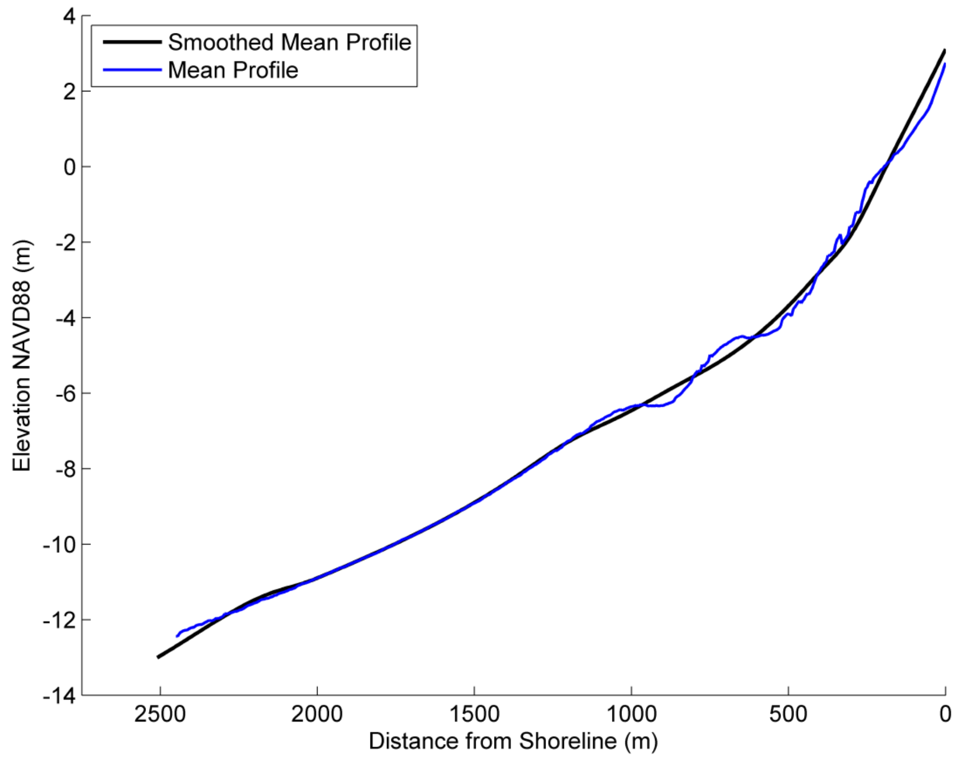

Figure 9. The mean profile in the CRLC often does not eliminate all bar features (blue line). Further smoothing is necessary to attain a bar-less profile that can be used for bar extraction. Features with wavelengths less than 500m are removed by the smoothing yielding the black line. Example from Long Beach, line 75.

Bars are initially identified as maximums and minimums in the perturbation profile (Figure 10). Based upon our estimated measurement error, the minimum perturbation from the mean we are able to confidently identify is approximately 0.2m; therefore only features that differ from the mean profile by at least 0.2m are extracted.

Due to differences in bar shape, the location of maximums in the perturbation profile is not always precisely at the local maximum of the bar. Because we consider the actual local maxima and minima of the profile to be the important morphological characteristic, we adjust the initial crest and trough positions to the local maxima and minima of the profile (Figure 10). Automatically extracted bar positions are all reviewed (and changed, if necessary) by an operator. An operator must approve each set of bar picks on a profile before the parameters are stored. Operators can change the automatic extraction by interactively choosing the bar crest and trough. We have used this method in the CRLC, where we have over a decade of survey data. For profiles with only one year of data, we could not define a mean profile; thus crests and troughs are picked as local maxima and minima along the profile itself. They are then reviewed and adjusted manually, if necessary. Our automatic extraction fails in situations where the bathymetry is complicated, such as rocky sections of coast. Extraction of nearshore terraces, discussed below, was often also accomplished manually.

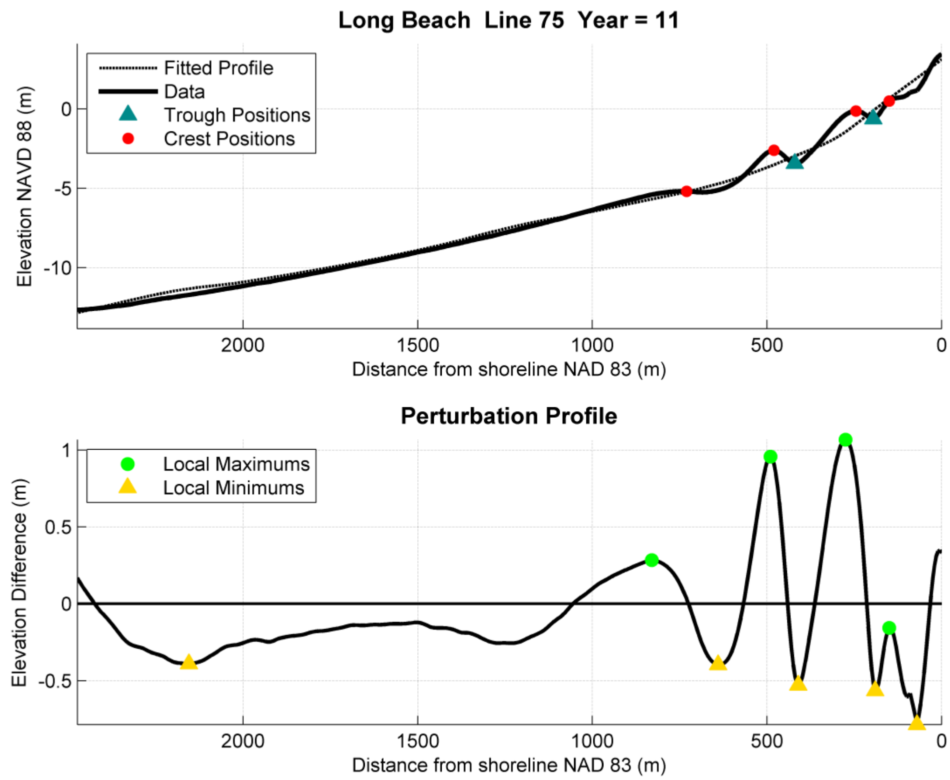

Figure 10. Interface used for sandbar extraction. Bottom: First, perturbations greater than 0.2m from the mean profile are identified. Top: Bar picks are then transferred to the bathymetry profile and verified by an operator. Extractions further from the shoreline than 1500m are automatically filtered out. Bar extraction without a mean profile identifies local maxima and minima from the data shown in the top panel.

We distinguish between sandbars, which have a distinct crest and trough, and nearshore terraces, which are characterized by inflections in the profile without a clear trough. Automatic extraction of these features requires a mean profile because the crest and trough can be recognized as a maximum and minimum in the perturbation profile without being such in the bathymetry profile (Figure 10). The definition of a bar requires that it not only have a crest and trough, but also that the trough elevation is lower than the crest elevation. For a terrace, on an upwardly sloping profile, this is not the case (see the seaward most bar in Figure 10). When a minimum in the perturbation profile is not associated with a trough in the bathymetry profile, the crest definition is changed from a local maxima to the point where the profile flattens into a step, or the point of maximum curvature (Figure 10). Automatic terrace extraction is not always successful in the CRLC because terrace crests are less distinct features of the profile than bar crests; for many cases in the CRLC and for all profiles with only one year of data, terraces were extracted manually by visually estimating the point where the profile flattens. While terraces and bars are defined differently in the extraction process by necessity, in the U.S. PNW, they are not distinct features. Any one bar may cycle in and out of a ‘terrace phase’ during its lifecycle or may display alongshore variability by existing as a bar and a terrace at the same time but in different locations. Once the features are picked there is no longer a distinction between bar and terrace crests. The same information on both is collected and stored, but terraces are distinguished from bars by a zero bar height.

The raw bar morphometrics were further refined to improve data quality for subsequent analysis. Because there is uneven coverage of the lower intertidal zone (approximately -1.5m to 1m), only subtidal bars (crest depth less than -1.5m) are considered here. In other cases, the entirety of a transect is eliminated from the analyses because it intersects a jetty or a headland rather than a sandy beach, and we are therefore unable to accurately determine a shoreline position. Compared to the number of bar picks eliminated from the intertidal zone, the number eliminated from transects around jetties and headlands is small. A total of 465 profiles out of 560 profiles and 552 bar picks out of 874 original bar picks were used for the spatial analysis.

3.4 Environmental Variable Data

We examine the alongshore variability of several environmental variables to improve our understanding of longshore variability in bar morphology. Parameters included the wave climate (wave height, period and direction), tide range, sediment grain size, upper shoreface slope, and foreshore beach slope (Wijnberg, 2002).

The upper shoreface slope influences wave shoaling, and thus can impact sediment transport in the nearshore. For the majority of data set the upper shoreface slope is defined between the position of the 2.1m (shoreline) and the -10m contours. Use of the -10m contour eliminates the influence of bar morphology on the slope; however the northern part of the North Beach cell is remarkably flat and our 2km long transects did not reach the -10m contour. In order to consistently compute the upper shoreface slope at -10m depth for the entirety of North Beach, we first computed the slope using the -7m contour, which was available at every transect. We then calculated the mean difference between the slope using the -7m contour and the slope using the -10m contour for the southern part of the littoral cell. The upper shoreface slope for the northern part of North Beach is the slope calculated using the -7m contour minus the mean difference of 0.0016 between the two slopes (Figure 11).

We calculated foreshore beach slope by interpolating through the all data points between the 1.6m and 2.6m contours. At least 5 data points were used for this interpolation. For bathymetry transects where there was no topography transect, we interpolated the 1.6m contour and 2.6m contour using the surrounding data with the same method as was used in the shoreline interpolation.

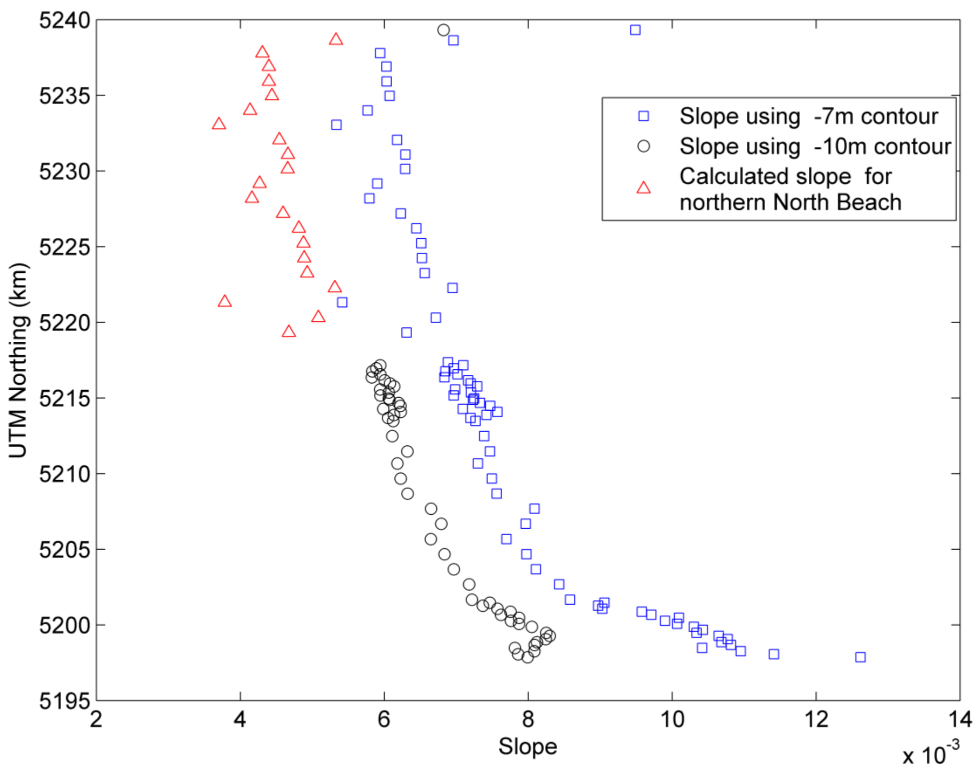

Figure 11. The upper shoreface slope, using the -10m contour, was calculated for northern North Beach using the upper shoreface slope at the -7m contour and the mean difference between the upper shoreface slope calculated using -10m and -7m in the southern part of the littoral cell.

The wave climate consists of the wave height, period, and direction. We characterized the wave climate using a 6 year hindcast obtained using both Wave Watch III v3.14 and Simulating WAves Nearshore (SWAN) v40.81 (Garcia-Medina et al., 2012). The hindcast provides significant wave height, mean wave period, mean wave direction, and peak wave direction for every hour of every day of the record at a model resolution of about 5km in the alongshore. We use the same definition of mean wave period, energy period, as that used by Garcia-Medina et al. (2012). The energy period represents the period at which most of the energy of the waves is transmitted. The regional patterns of energy period are similar to other definitions of mean wave period. Wave direction is given in the azimuth coordinate system. We reverse shoaled the significant wave height in 50m of water to deep water using linear wave theory and also estimated breaking wave height using the method of Komar and Gaughan [1976].

$$H_b = 0.39 g^{1/5} (T H_o^2)^{2/5} \quad (1)$$

Tide range affects the depth of water over a bar, and thus affects whether waves are breaking on the bars. We used 1 year (2011) of tide predictions from 4 NOAA operated tide gauge stations in the study area (Garibaldi, OR, Hammond, OR, Toke Point, WA, and Westport, WA). Using tide predictions instead of gauge measurements allowed us to avoid data gaps as well as the effects of storm surge and other non-astronomical water level components. Gauge stations in the PNW are typically located in estuaries. To minimize the complex effects of estuaries on tides, these stations were chosen to be as close as possible to the open coast.

Sediment grain size influences how easily sediment is transported as well as bedform evolution. Grain size data for the study area was obtained from Peterson et al. (1994). The grain size data includes the mean diameter and the standard deviation of the intermediate grain axis. The standard deviation is a measure of sorting. The samples are mid-beach samples taken from within 10cm of the surface. There is approximately 1 data point per 5km in the study area.

4 Results

In this section we discuss regional, inter-littoral cell trends and variability in sandbar morphometric parameters and environmental variables. The range and distribution of variability of each is discussed.

4.1 Morphometric Parameters

There is considerable alongshore variability in the bar position from the shoreline, bar crest depth, and bar height, both within and among littoral cells (Figure 12). From north to south, the maximum and mean bar positions show a regional trend of decreasing distance from the shoreline (Table 2). Bars in the CRLC and Cannon Beach are much more widely distributed over the nearshore zone than in Rockaway, Netarts, and Neskowin. Bar positions range from 200m to 1000m from the shoreline in the most northerly five littoral cells (the CRLC and Cannon Beach), while in the next three littoral cells to the south (Rockaway, Netarts, and Neskowin) the bars exist primarily between 200m and 600m from the shoreline (Table 2). Here we define the maximum range of bar position for the entirety of a littoral cell as the effective bar zone. Bars in the CRLC and Cannon Beach have a wider effective bar zone than in Rockaway, Netarts, or Neskowin (Figure 12; Table 2). The width of the effective bar zone decreases from over 800m in the CRLC to less than 400m in Rockaway and Netarts. T-tests confirm that the CRLC mean bar positions are greater than the mean bar positions in Rockaway, Netarts, and Neskowin, giving us added confidence that the trend in width of effective bar zone is real (Table 3).

An intriguing consequence of narrower effective bar zones appears to be a transition from a multiple barred system in the CRLC and Cannon Beach to a single barred system in Rockaway, Netarts, and Neskowin (Figure 12). Individual transects in the CRLC and Cannon Beach are much more likely to contain two or more subtidal bars than transects further south. This tendency can most easily be seen in Long Beach, Clatsop Plains, and Cannon Beach (Figure 12). Frequency distributions of bar positions in each littoral cell illustrate variability in bar position and number of subtidal bars (Figure 13). The CRLC and Cannon Beach have multiple peaked distributions for bar position, clearly displaying a tendency towards multiple barred systems. While the distribution in Long Beach suggests a triple bar system exists, the rest of the CRLC and Cannon Beach show a double barred system. The bar position distributions of Rockaway, Netarts, and Neskowin have a single peak which is consistent with a single barred system.

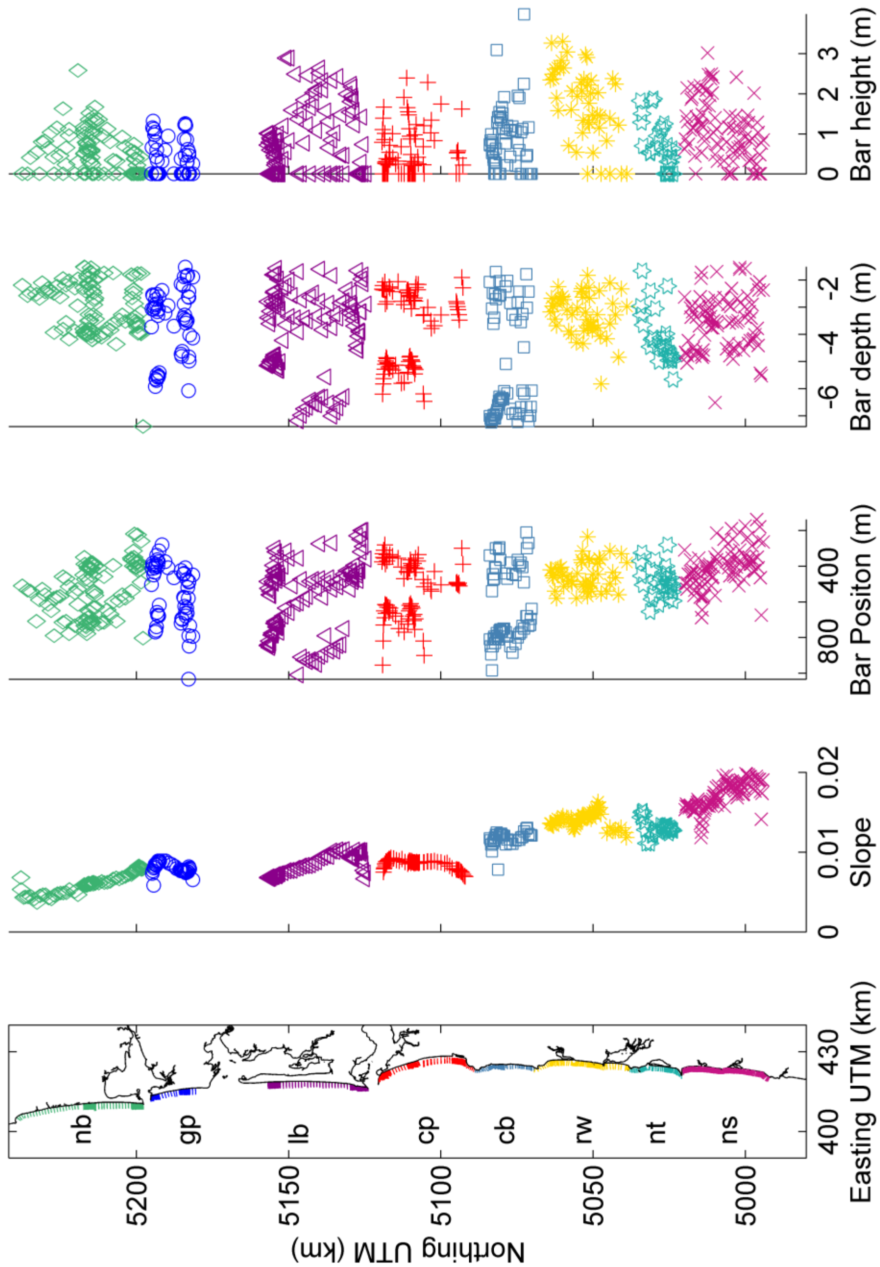

Figure 12. Summary of bar morphometric parameters separated by littoral cell. Each transect is plotted along the shoreline in panel 1. Littoral cells are labeled with their assigned abbreviation. Panel 2 shows the variability of slope in space. Panels 3 through 5 show the variability of each of the morphometric parameters through the study area. Each littoral cell is represented by the color and symbol indicated in Figure 1.

Table 2 Bar Position Statistics

Littoral Cell	Minimum distance from shoreline (m)	Maximum distance from shoreline (m)	Width of effective bar zone (m)	Mean distance from shoreline (m)	Median distance from shoreline (m)	Std (m)
North Beach	220	805	585	540	540	150
Grayland Plains	280	1035	755	550	505	165
Long Beach	200	1010	810	575	500	205
Clatsop Plains	280	955	670	535	505	160
Cannon Beach	210	985	766	625	735	210
Rockaway	235	580	345	450	455	80
Netarts	280	655	375	485	500	90
Neskowin	140	690	550	405	410	110

Table 3. T-Test for bar position compares the means for each littoral cell against every other littoral cell. = indicates that the means are equal; < denotes that the mean of X is less than the mean of Y; > indicates that the mean of X is greater than the mean of Y. Littoral cells are abbreviated along the top row as follows: North Beach – nb; Grayland Plains – gp; Long Beach – lb; Clatsop Plains - cp; Cannon Beach - cb; Rockaway – rw; Netarts – nt; Neskowin - ns

Y	X →							
	nb	**gp**	**lb**	**cp**	**cb**	**rw**	**nt**	**ns**
North Beach	-							
Grayland Plains	=	-						
Long Beach	=	=	-					
Clatsop Plains	=	=	=	-				
Cannon Beach	<	<	=	<	-			
Rockaway	>	>	>	<	>	-		
Netarts	>	=	>	=	>	=	-	
Neskowin	>	>	>	>	>	>	>	-

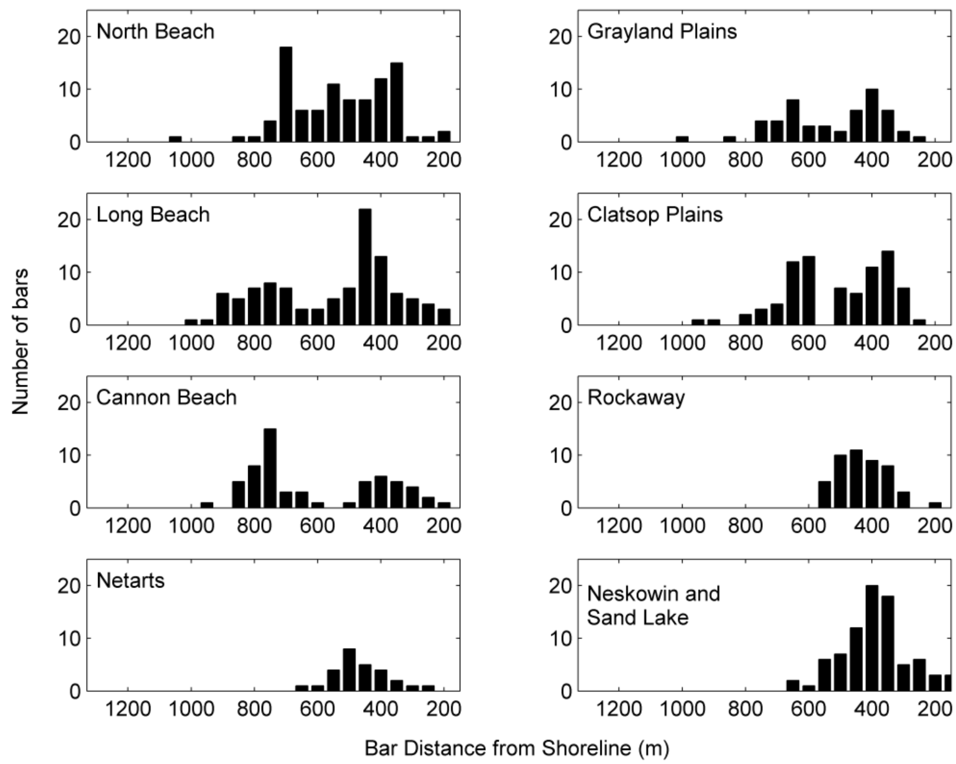

Figure 13. Histograms of bar positions within each littoral cell document a transition from multiple barred systems to single barred systems. Bins are 50m wide.

In contrast to the longshore variability in bar position, bar depths are more consistent in the alongshore (Figure 12). The depth limit across the study area is approximately 7m (Table 4); only 3% of bar crests in the study area are deeper than 7m. The majority of the bars are shallower than 5m in every littoral cell, except for Cannon Beach. There is no clear regional longshore trend in the maximum bar depth or depth range of the effective bar zone. Maximum depths within each of the littoral cells range from 5.8m to 7.4m. Distributions of the bar depths for each littoral cell show similar results to the position distributions in that there is a tendency for profiles to have multiple bars in the CRLC and Cannon Beach and a single bar in Rockaway, Netarts, and Neskowin (Figure 14). Cannon Beach has the deepest mean depth; this is due to a higher occurrence of bars in the deeper part of the depth range rather than Cannon Beach exhibiting a larger depth range. The maximum depth in North Beach is due to one anomalous bar near the Grays Harbor jetty; without that bar the maximum depth in North Beach is 4.4m. The bar crest depth histogram of North Beach has more similarities, in terms of depth range, with Rockaway, Netarts, and Neskowin. T-tests indicate that the mean depths in Grayland Plains, Long Beach, Clatsop Plains, Cannon Beach, and Neskowin are not statistically different from each other, lending support to the lack of a regional trend in bar depth (Table 5).

Table 4. Bar Depth Statistics

Littoral Cell	Maximum bar depth (m)	Minimum bar depth (m)	Depth range of effective bar zone (m)	Mean bar depth (m)	Median bar depth (m)	Std
North Beach	7.4	1.5	5.9	3.0	2.9	1.0
Grayland Plains	6.1	1.5	4.6	3.6	3.2	1.3
Long Beach	7.2	1.6	5.6	3.9	3.4	1.5
Clatsop Plains	6.5	1.9	4.6	3.8	3.3	1.4
Cannon Beach	7.2	1.7	5.5	5.1	6.2	2.0
Rockaway	5.8	1.8	4.0	3.3	3.2	0.8
Netarts	6.8	1.7	5.1	4.1	4.4	1.0
Neskowin	6.5	1.5	5.0	3.6	3.5	1.0

Table 5. T-Test for bar depth compares the means for each littoral cell against every other littoral cell. = indicates that the means are equal; < denotes that the mean of X is less than the mean of Y; > indicates that the mean of X is greater than the mean of Y. Littoral cell abbreviations are the same as in Table 3.

Y	**X →**							
	nb	**gp**	**lb**	**cp**	**cb**	**rw**	**nt**	**ns**
North Beach	-							
Grayland Plains	<	-						
Long Beach	<	=	-					
Clatsop Plains	<	=	=	-				
Cannon Beach	<	<	<	<	-			
Rockaway	-	=	>	>	>	-		
Netarts	<	<	=	=	=	<	-	
Neskowin	<	=	=	=	=	=	>	-

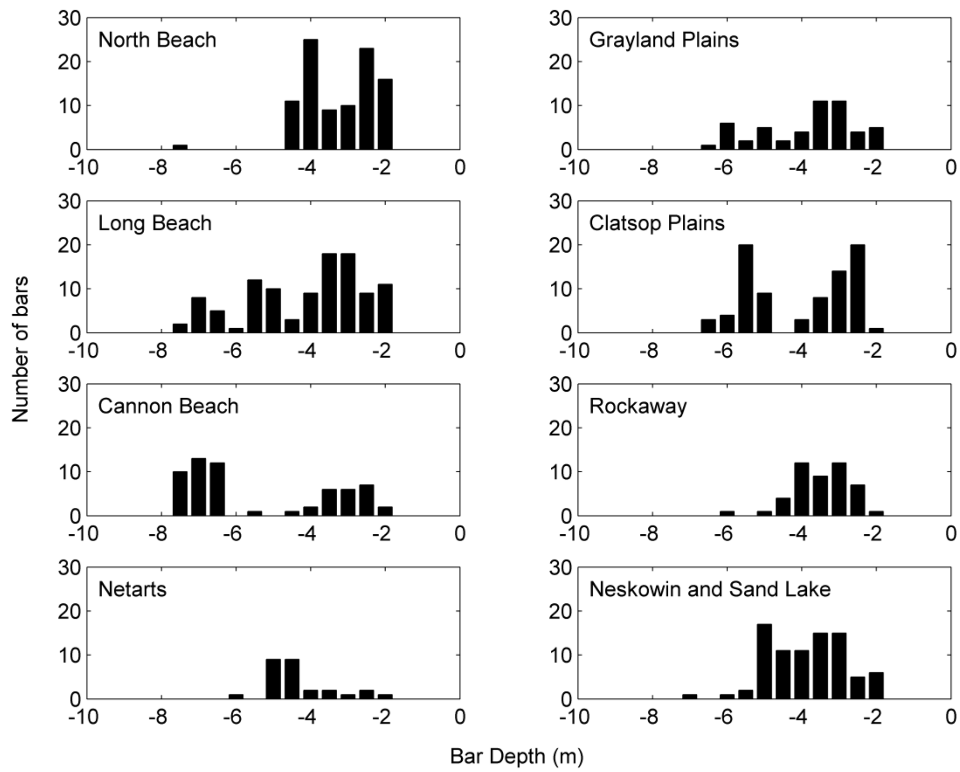

Figure 14. Histograms of bar depth for each littoral cell. A transition from multiple bars per profile to a single bar per profile is observed. All littoral cells share a similar maximum depth. Bin widths are 0.5m.

Ninety percent of the bars in the study area are less than 2m in height and 65% are less than 1m in height. Terraces make up 28% of the extracted bars. Although bar height does not exhibit regional longshore trends in terms of maximum bar height, there is some alongshore structure in the frequency of terrace occurrence (Figure 12; Table 6). For instance, 46 % of the bars in Rockaway are greater than 2m in height, and only 16% are terraces. In contrast, in Grayland Plains there are not any bars greater than 2m in height and 49% of the bars are terraces. The percent of terraces in each littoral cell clearly distinguishes the CRLC from the rest of the study area (Table 6), with terraces characterizing 38% of the CRLC bars. Each subcell of the CRLC has a higher percentage of terraces than the study area as a whole, while each of the other littoral cells has a lower terrace percentage than the data set as a whole. In addition, the CRLC has an overall higher frequency of smaller bars compared with Cannon Beach, Rockaway, Netarts, and Neskowin (Figure 15). Outside the CRLC, the bar height distributions are broadly distributed. T-tests demonstrate that there is substantial variability in the mean bar height throughout the region (Table 7). Rockaway has the largest mean bar height in the region, followed by Neskowin and Cannon Beach which do not differ significantly in mean bar height.

Table 6. Bar Height Statistics. Mean bar heights in parentheses represent the mean without the zero heights associated with nearshore terraces.

Littoral Cell	Maximum bar height (m)	Mean bar height (m)	Median bar height (m)	Std (m)	Percent terraces
North Beach	2.6	0.5 (0.8)	0.5	0.5	34
Grayland Plains	1.3	0.4 (0.7)	0.2	0.4	49
Long Beach	2.9	0.8 (1.3)	0.7	0.8	34
Clatsop Plains	2.4	0.5 (0.8)	0.3	0.6	33
Cannon Beach	4.0	0.8 (1.1)	0.8	0.8	22
Rockaway	3.3	1.8 (1.9)	1.9	0.9	11
Netarts	1.9	0.7 (0.9)	0.6	0.6	22
Neskowin	3.0	1.1 (1.2)	1.1	0.7	10

Table 7. T-Test for bar height compares the means for each littoral cell against every other littoral cell. = indicates that the means are equal; < denotes that the mean of X is less than the mean of Y; > indicates that the mean of X is greater than the mean of Y. Littoral cell abbreviations are the same as Table 3. Means were computed without 0 values for bar height.

Y	X →							
	nb	**gp**	**lb**	**cp**	**cb**	**rw**	**nt**	**ns**
North Beach	-							
Grayland Plains	=	-						
Long Beach	<	<	-					
Clatsop Plains	=	=	>	-				
Cannon Beach	<	<	=	<	-			
Rockaway	<	<	<	<	<	-		
Netarts	=	=	>	=	=	>	-	
Neskowin	<	<	=	<	=	>	=	-

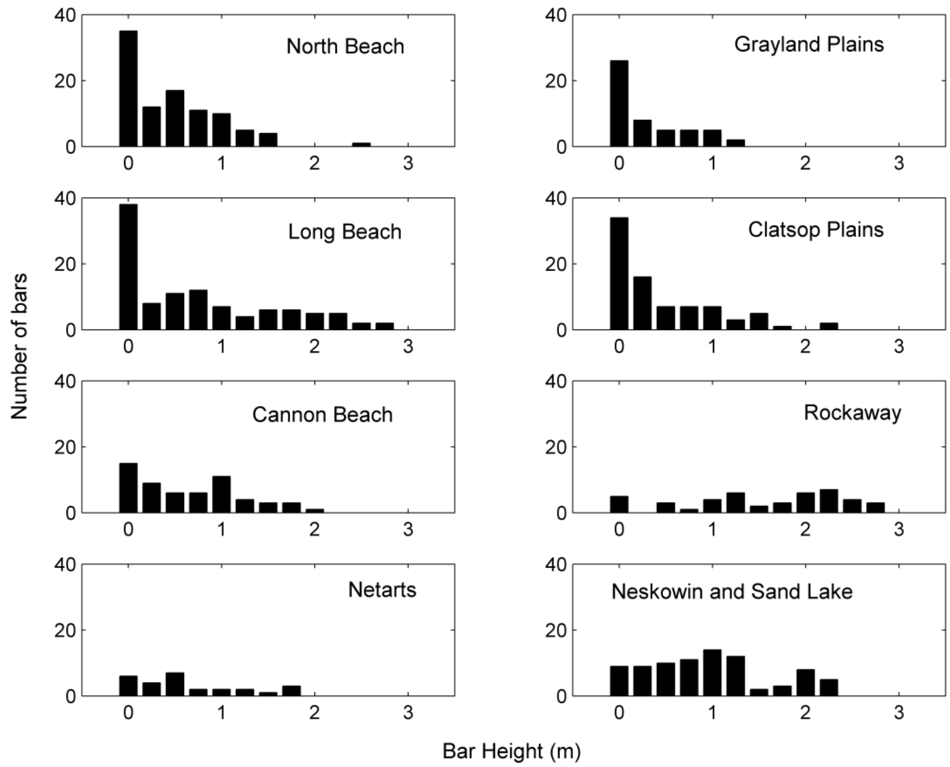

Figure 15. Histograms of bar height for each littoral cell. Bin widths are 0.25m.

4.2 Environmental Variables

The following section discusses the variability of the upper shoreface slope, wave climate, grain size, and tides through the study region.

4.2.1 Upper shoreface slope

A striking regional trend in upper shoreface slope exists through the study area (Figure 12; panel 2). The slope ranges from 0.0053 (~1:200), in North Beach, to 0.0205 (~1:50), in Neskowin, a change of almost a factor of 5 over approximately 250km. The north to south steepening trend shows an abrupt shift towards a higher slope at Tillamook Head. The upper shoreface slope partitions the CRLC from Cannon Beach, Rockaway, Netarts, and Neskowin.

Within the regional trend, there are also smaller intra-littoral cell trends within the CRLC. The upper shoreface slope steepens towards Grays Harbor and the Columbia River Mouth (MCR), both jettied estuary mouths. The same trend is not seen around Willapa Bay; however the area where we would expect to observe the trend is the area where we have a gap in data coverage due to the ebb tidal delta. Similar intra-littoral cell trends are not readily observed south of the CRLC.

4.2.2 Wave climate

Wave height, wave period, and wave power vary in the alongshore as a response to local wave transformations over the variable bathymetry, but a regional trend is not apparent (Figure 16). Mean wave direction (MWD) shows substantial regional longshore variability (Figure 16). The MWD ranges from an average of 267°, in an azimuth coordinate system, to an average of 279°, indicating a shift from a southwesterly approach to a northwesterly approach. There is a substantial difference between the MWD of summer waves and winter waves. The average difference in the region is 8.3°. Individual bars often survive for multiple years and therefore, their characteristics are influenced by the cumulative effects of the wave and current conditions over a multi-year timescale. Considering this, we chose to represent the wave climate variables with annual average conditions.

Despite the longshore trend in MWD, the longshore component of wave power does not exhibit a longshore regional trend (Figure 17). Cumulative longshore wave power was computed by summing the longshore component of wave power at each output point of the wave hindcast record. Positive power refers to northward directed power, and negative power refers to southward directed power. In order to look at the regional and intra-littoral cell trends, we averaged the longshore wave power at 5km intervals within each littoral cell.

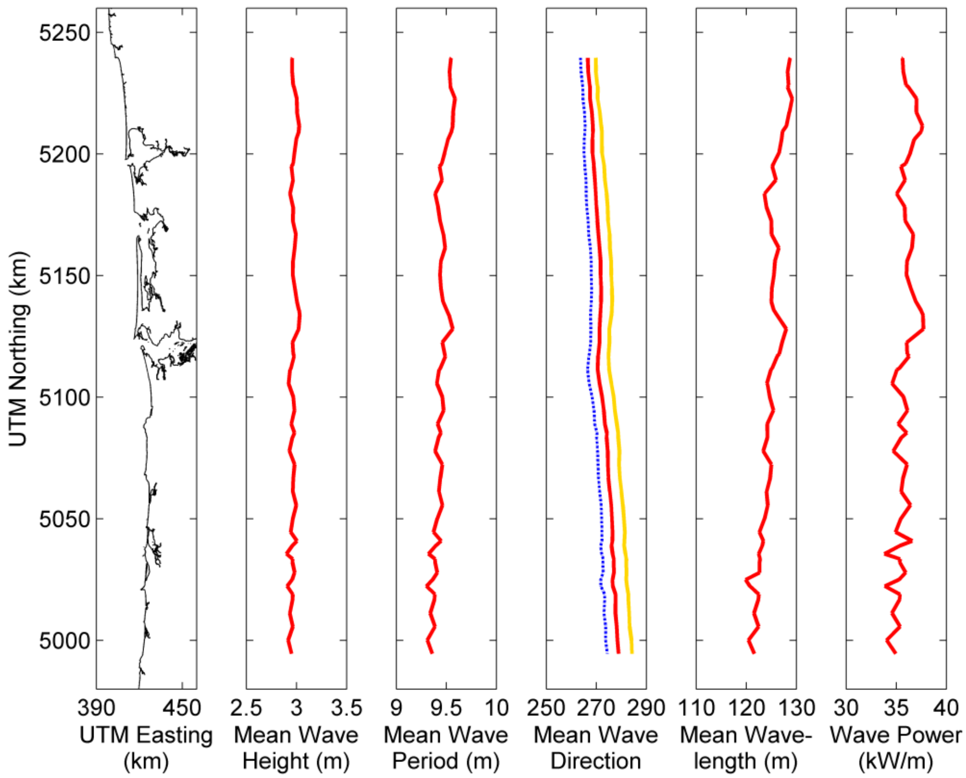

Figure 16. Longshore variability in the wave climate as computed from the hindcast. Means are computed over the entirety of the data record and for breaking wave conditions unless otherwise specified. Mean wave direction (MWD) is shown for summer (yellow), winter (blue dashed), and entire record (red). Mean wave direction is in an azimuthal coordinate system with waves at 270 coming from due west. Mean wave direction and mean wavelength are shown at 50m depth.

Net northward power is more common overall in the study area (Figure 17). Southward directed wave power is often associated with northwest shoreline orientations found in the CRLC. Longshore power in both North Beach and Clatsop converges toward the center of the littoral cell. Grayland and Long Beach have uniform directions, but display decreasing magnitude towards the entrance to Willapa Bay (Figure 17). South of the CRLC the longshore power is directed almost exclusively to the north. There are relatively smaller changes in magnitude south of the CRLC.

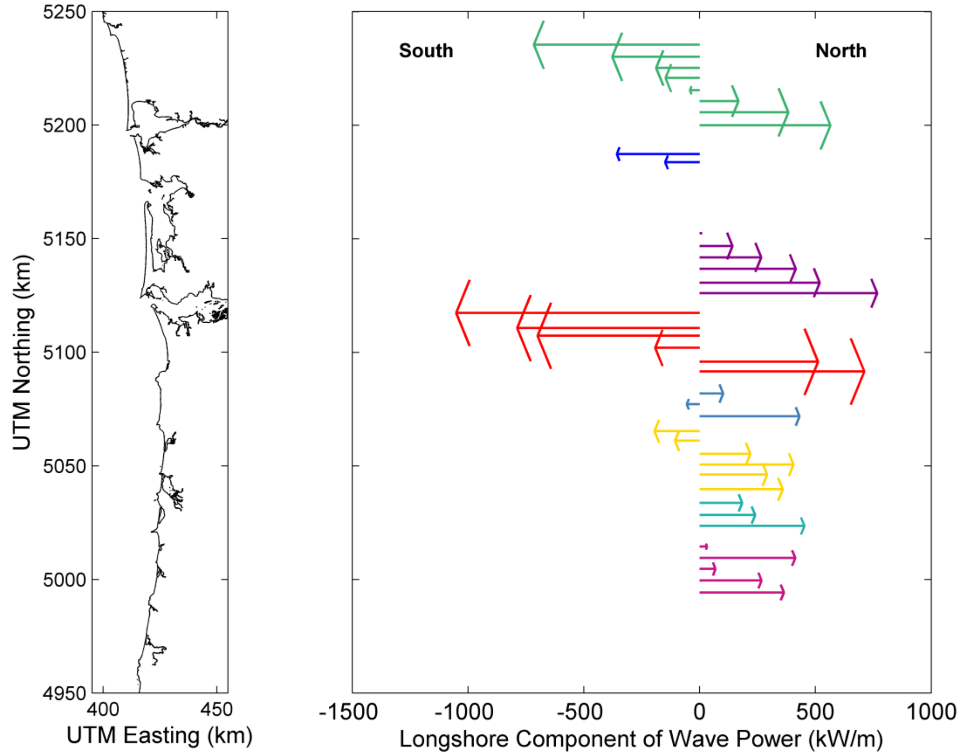

Figure 17. Cumulative longshore wave power was computed over the entire 6 year wave record. Values are 5km longshore averages within each littoral cell. The length of the arrow represents the magnitude of the power multiplied by 10^{-3}. Colors correspond to the previously defined color scheme for the littoral cells.

4.2.3 Grain size

Throughout the study area the beaches are composed of very fine to medium sand (Figure 18). The majority of the sediment is fine sand in the range of 0.125mm to 0.25mm. The range of sediment sizes, represented by the standard deviation about the mean, is small, indicating well sorted sands (Figure 18). The degree of sorting is highest at the far north end of the study area and lowest at the far south end; however there is no trend in sorting through the middle of the study area.

Two regional scale longshore trends are apparent. First, within the CRLC, sediment fines away from the Columbia River (Kaminsky et al., 2010). Mean grain sizes within Long Beach and Clatsop are 0.24mm and 0.20mm, respectively, while mean grain sizes in Grayland and North Beach are 0.18mm and 0.16mm, respectively. Second, grain size coarsens south of Tillamook Head. The mean grain sizes for Cannon Beach, Rockaway, Netarts and Neskowin 0.17 mm, 0.19, 0.17, and 0.32mm, respectively.

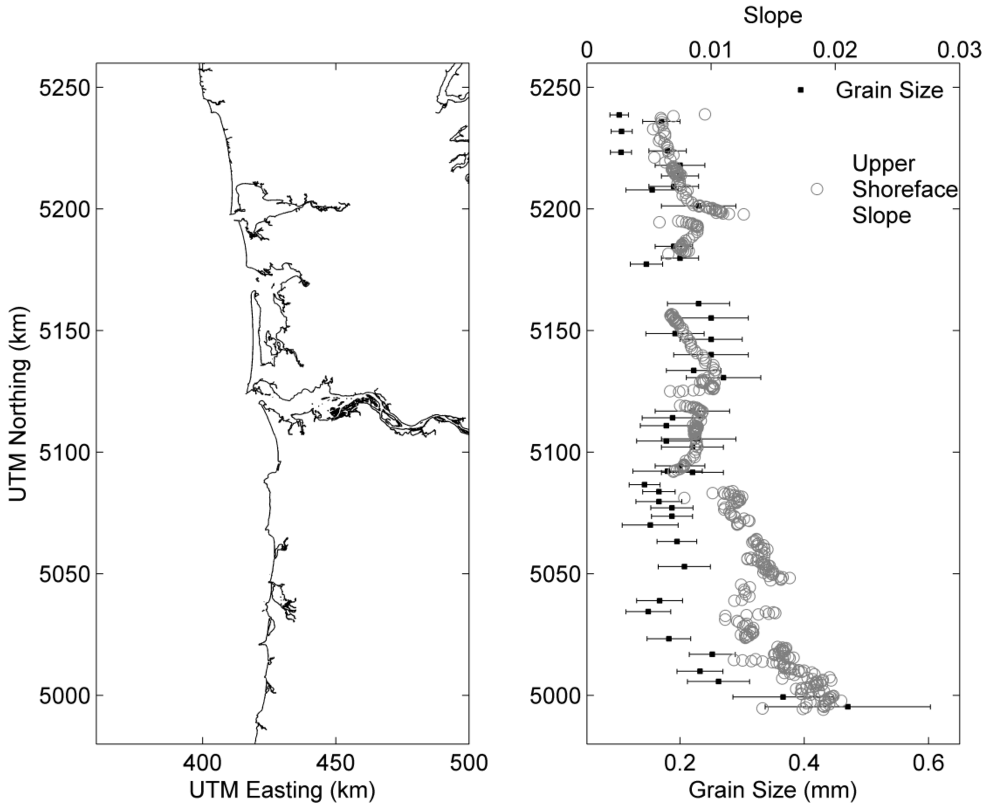

Figure 18. Regional variations in the mean grain size with error bars showing sorting using the standard deviation about the mean.

4.2.4 Tides

The range of spring tides in the study area show very low variability. The highest mean spring tide range within the study area is 3.3m and the lowest is 3.1m. The highest mean neap tide range is 0.9m and the lowest is 0.7m.

5 Discussion

We have thus far considered the presence and absence of longshore, regional trends in bar morphometric parameters as well as several environmental variables. In the following section we consider the importance and significance of those trends for regional-scale bar morphology. We first consider the relationships between environmental variables and morphometric parameters. We then compare the spatial variability of the CRLC data with its temporal variability in order to explore the range of variability seen in each. Finally, we discuss the morphology, occurrence, and behavior of nearshore terraces in the data set.

5.1 Relating Changes in Bar Morphometrics to Changes in Environmental Variables

As the upper shoreface slope increases southward through the study area there are noteworthy changes in the bar position characteristics: the width of the effective bar zone decreases, the mean bar position decreases, the maximum bar position decreases, and there is a transition from a predominance of multiple bars per profile to a single bar per profile. Upper shoreface slope is significantly correlated with the maximum and mean bar position (Table 8). The position of the outer bar is also significantly correlated with the upper shoreface slope (Figure 19). In contrast, the range of depths through which bars are observed does not vary with the upper shoreface slope (Figure 19). Instead, there is a regional limit to bar depth at approximately -7m. While the mean depth is not significantly correlated with any of the tested environmental variables, the depth range is significantly correlated with breaking wave height and wavelength (Table 8).

A potential physical explanation of the observed correlations with position and depth range is that the bar zone is influenced by the zone of breaking waves. CRLC beaches are exceptionally flat and dissipative, with very wide zones of breaking waves. As slope increases through the study region, but breaking wave height remains essentially the same, beaches become less dissipative and the zone of breaking waves narrows. It is not a coincidence that a narrower zone of breaking waves results in a narrower effective bar zone. Bars will only occur in the profile where there are significant gradients in sediment transport. Waves, wave induced currents, and especially, breaking waves are responsible for much of the sediment movement in the nearshore zone. Thus we should expect that the width and location of the bar zone is influenced by the width and location of the breaker zone.

An explanation for the relationship between the upper shoreface slope and the number of bars per transect is less clear. An increased slope does not necessarily lead to the transition from a multiple bar system to a single bar system. The distance between successive bar crests could decrease to accommodate multiple bars in a narrower area; however that is not what we observe. Bar size is a likely constraint on the separation distance between bar crests; however we find no relationship between bar height and any of the environmental variables. Future investigations could focus on characterizing bar size in other ways (eg. bar volume) to explore the possibility of a relationship between bar size and number of bars per profile.

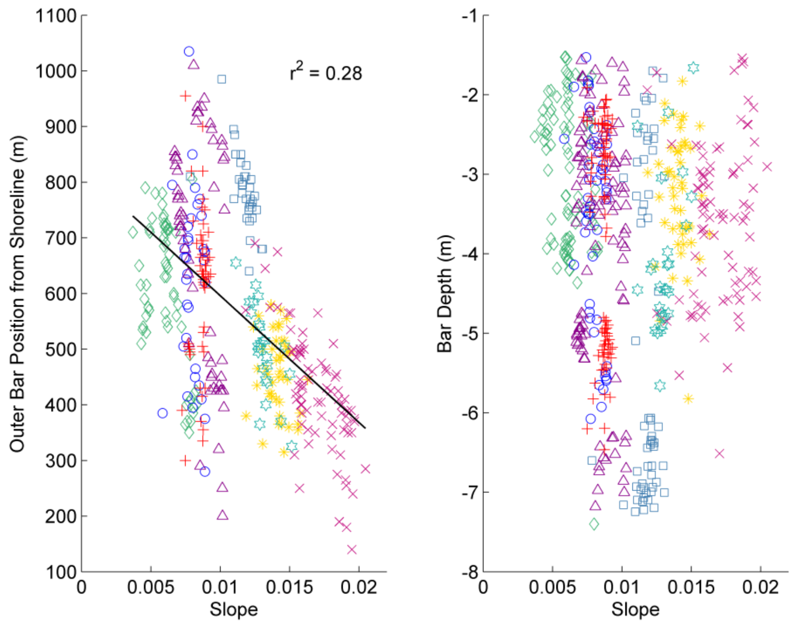

Figure 19. The relationship between upper shoreface slope and outer bar position and depth with all littoral cells represented by their respective colors and symbols indicated in Figure 1. The relationship between slope and outer bar position is significant at the 95% confidence level.

Ruessink et al. (2003) investigated the relationships between bar morphometrics and environmental characteristics using data from Duck, North Carolina, Hasaki, Japan, and four sites from the Dutch coast. Their study focused on intersite differences in NOM behavior characterized by sandbar morphometrics. Linear regression analysis of bar morphometric parameters with bulk environmental variables suggested that the bar depth range tended to increase with the breaking wave heights of storms; however, overall the results were inconclusive because the magnitude of the correlation was often strongly influenced by individual sites. Linear regression analysis of data from the PNW also indicates that the bar depth range is influenced by breaking wave height (Table 8). While Ruessink et al. (2003) found considerable intersite differences in mean bar depth, we find that depth is the most spatially consistent morphometric parameter in the PNW.

The Cannon Beach littoral cell is similar to the CRLC in some aspects of beach morphology and similar to Rockaway, Netarts, and Neskowin in others. Cannon

Beach shares similar bar position characteristics with the CRLC and also displays a two bar system; however in terms of sediment characteristics, slope trends, and percentage of terraces, Cannon Beach is more similar to Rockaway, Netarts, and Neskowin. The mixed characteristics of Cannon Beach suggest that no single environmental variable can explain all of the variability seen through the study area. Sandbar morphology, and the variability of that morphology, results from the interaction of multiple environmental factors.

To further investigate possible relationships between bar morphology and environmental forcing, we calculate three non-dimensional parameters, the Iribarren number, the dimensionless fall velocity, and the Relative Tide Range. Non-dimensional quantities are often used to compare the collective influence of multiple processes on morphology, and are useful parameters for comparing the influence of environmental variables on areas with disparate characteristics. Often general guidelines for the behavior of a process, based on ranges of a non-dimensional quantity, can be developed into a classification system. For instance, the Iribarren number relates slope and wave steepness and can be used to speculate about breaker type. We use an Iribarren number-like parameter,

$$\xi = \frac{S}{\left(\frac{H_b}{L_0}\right)^{\frac{1}{2}}} \qquad (2)$$

where S is upper shoreface slope, H_b is breaking wave height, and L_0 is deep water wavelength. Iribarren number is traditionally calculated using the deep water wave height and beach slope. Here we use breaking wave height because we are interested in surf zone processes and upper shoreface slope because we are considering only subtidal morphology, and it is therefore the more relevant slope for shoaling and breaking processes. The relationship between slope and wave steepness describes how much of the energy of a breaking wave is reflected and how much is dissipated. Lower Iribarren numbers suggest more energy dissipation. The amount of energy dissipated by a breaking wave and the breaker type influences sediment stirring and transport (Smith et al., 2009). Dimensionless fall velocity (Ω), also known as the Dean

Parameter, (Masselink and Short, 1993) is a relationship between wave steepness and sediment size,

$$\Omega = \frac{H_b}{w_s T} \quad (3)$$

where w_s is settling velocity, and T is wave period. Ω greater than 2 suggests the dominance of offshore sediment transport and barred profiles while Ω less than 2 suggests the dominance of onshore sediment transport and berm type profiles (Masselink and Hughes, 2003). The relative tide range (RTR) expresses the relative importance of shoaling, surf zone, and swash processes along a beach.

$$RTR = \frac{mean\ spring\ tide\ range}{H_b} \quad (4)$$

The RTR influences the location of the surf zone with respect to the profile. As RTR increases, more of the profile is subject to shoaling processes over a tidal cycle, and these processes become more influential for morphology (Masselink and Short, 1993).

The non-dimensional environmental parameters display minimal longshore variability in the study area (Figure 20). Iribarren number varies between 0.033 and 0.12. Breaker type tends to change with an Iribarren number around 0.4, signaling a significant change in how much energy is dissipated. Dimensionless fall velocity (Ω) displays more longshore variability than the other dimensionless quantities. The dimensionless fall velocity ranges from 5.6 to 48; however, it is not clear how the change in magnitude affects morphology. The RTR displays very low variability, with values between 1.0 and 1.1 (Figure 20). The Iribarren number and RTR are both significantly correlated with bar morphometric parameters (Table 8). The correlations shown with Iribarren number are believed to be a result of the correlation of slope with bar morphometrics because the slope shows much greater variability than either wave height or wavelength. The correlation between RTR and maximum bar position suggests that as RTR increases bars are found further from the shoreline; however we interpret this correlation with caution because the tide range is characterized by only four points.

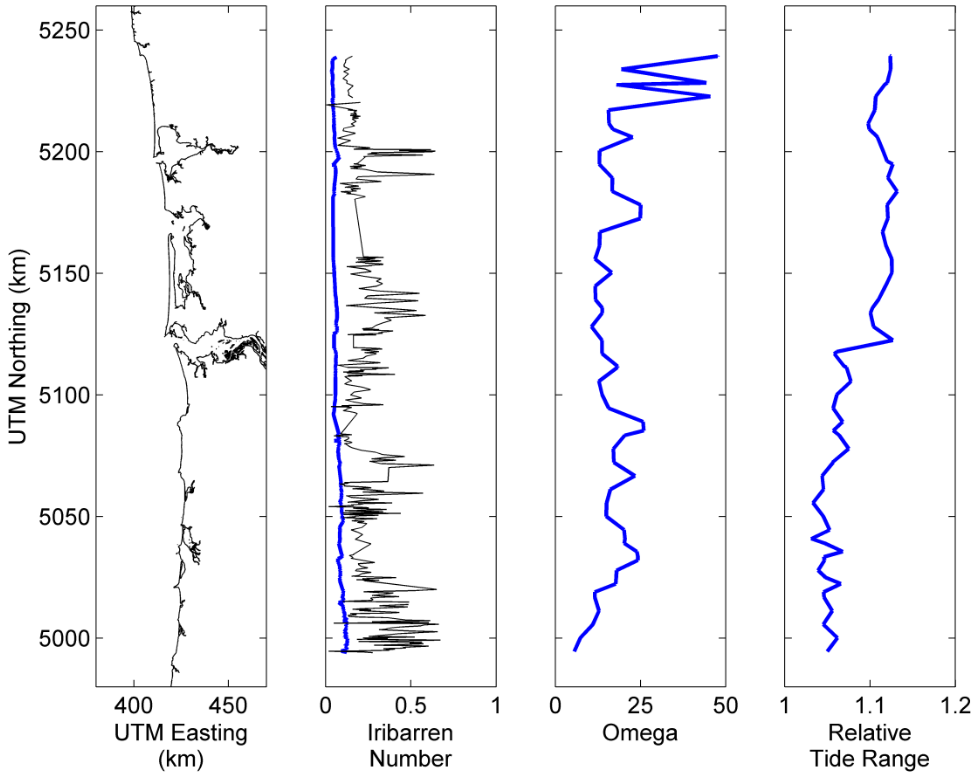

Figure 20. Longshore changes in Iribarren number, dimensionless fall velocity, and relative tide range. Iribarren number calculated with foreshore beach slope (black) and upper shoreface slope (blue) are compared. Longshore variability in the sediment size of northern North Beach causes the variability in dimensionless fall velocity.

Table 8. Correlations for environmental variables and bar morphometric parameters. Correlations that are significant at the 95% confidence level are bold and blue.

	Effective Width of Bar Zone	Maximum Position	Mean Position	Mean Depth	Depth Range	Mean Height
Slope	-0.64	**-0.78***	**-0.74***	0.54	-0.15	0.11
Grain Size	0.029	-0.18	-0.56	0.26	-0.15	-0.15
Breaking Wave Height	0.40	0.31	0.48	0.30	**0.77**	-0.17
Wave Period	0.51	0.51	0.61	-0.16	0.61	-0.28
Mean Wavelength	0.41	0.33	0.50	0.24	**0.77**	-0.20
Wave Direction	-0.62	-0.70	-0.62	0.52	-0.24	0.33
Wave Power	0.54	0.50	0.60	0.10	0.68	-0.18
Longshore Component of Wave Power	-0.28	-0.41	-0.10	0.55	0.63	0.24
Spring Tide Range	0.70	0.71	0.57	-0.38	0.37	-0.28
Iribarren Number	-0.64	**-0.78***	**-0.74***	0.54	-0.15	0.11
Dimensionless Fall Velocity	-0.15	-0.027	0.33	-0.29	0.43	-0.20
Relative Tide Range	0.70	**0.73**	0.54	-0.48	0.25	-0.28

*Slope and Iribarren number are strongly correlated.

5.2 Temporal Variability

In order to put the variability of our regional scale, spatial data set of sandbar morphology in context of the temporal variability in the study are, we extracted sandbars at four 1km long sections of coast for which we have at least 13 years of data (Figure 21; Table 9). These data allow us to begin to consider how well a single, large-scale measurement of sandbar morphology represents the full range of bar morphology seen over the NOM cycle. The NOM cycle in the PNW is thought to be on the order of 4 to 6 years, but has not yet been definitively determined and is still an area of active research. From the temporal sandbar data we ask the question: does a regional scale data set of spatial variability, at one time slice, show the same statistics of bar morphology as those computed over a long temporal scale, limited spatial scale data set?

The long temporal scale data set considered here consists of 6 profiles (1km) in each of North Beach, Grayland Plains, Long Beach, and Clatsop Plains. We chose the profiles to maximize record length and also avoid jetties and headlands. The profiles in North Beach, and Long Beach have 15 years of data from 1998 to 2012. The Clatsop Plains profiles cover the same time period, but are missing 2004 and 2012. The profiles in Grayland Plains have 14 years of data (1999 – 2012). We use the same morphological parameters and quality restrictions used with the regional scale data set to characterize the temporal variation. There are 554 bars used out of 750 extracted (Table 9). The statistics of each littoral cell determined from the temporal data set are compared to those from the same littoral cell determined from the spatial data set.

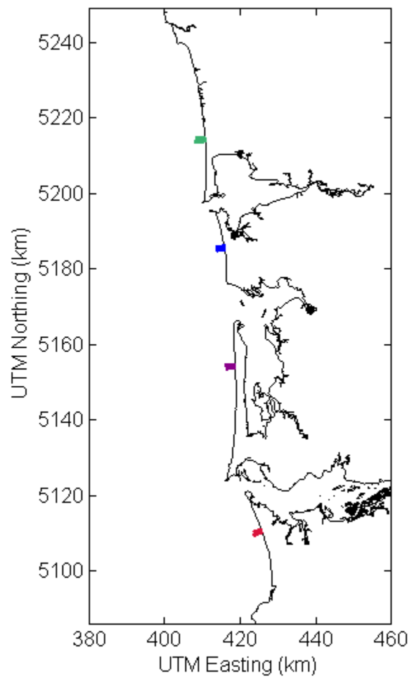

Figure 21. Map showing the CRLC profiles used for the temporal-spatial comparison. Each block of color represents 6 profiles and 1km of measurements.

Table 9. Temporal Data Set Summary

Littoral Cell	Number of years	Number of bars extracted	Percent Terraces
North Beach	15	133	41
Grayland Plains	14	113	48
Long Beach	15	166	28
Clatsop Plains	13	142	27

The temporal data considered here show similar statistics of morphometric parameters when compared to the spatial data (Table 10; Figure 22; Table 11; Figure 23; Table 12; Figure 24). The mean values for each morphometric parameter are the most consistent across data sets, while the maximums and minimums are more variable. Bar crest depth was the most consistent morphometric parameter in both time and space (Table 11). The depth range of the effective bar zone is also similar in time and space. Mean bar heights in North Beach, Grayland Plains, and Long Beach from the temporal data set are consistent with those from the spatial data set (Table 12). T-tests suggest that mean bar depths and mean bar positions for each subcell are, in general, not statistically different in time and space (Table 13). Mean bar heights are more variable.

One of the more striking changes through the study region is a transition from transects that predominantly have multiple subtidal bars per profile to transects that predominantly have a single bar per profile. Because the number of bars per profile might change through the NOM cycle, we compare the number of years for which each littoral cell displays a multiple bar system to the number of years for which it displays a single bar system (Table 14). To be classified as a multiple bar system at least half of the profiles must show at least 2 bars. Along this particular section of each littoral cell, North Beach and Grayland Plains display a single bar system about as often as a multiple bar system. Long Beach and Clatsop Plains display a multiple bar system about twice as often as a single bar system. Based on these results, the observed spatial trends, though capturing significant amounts of sandbar variability, should not be considered to be a complete characterization of sandbar variability over the entirety of the NOM cycle.

Table 10. Temporal Bar Position Statistics

Littoral Cell	Minimum distance from shoreline (m)	Maximum distance from shoreline (m)	Width of effective bar zone (m)	Mean distance from shoreline (m)	Median distance from shoreline (m)	Std (m)
North Beach	300	900	600	545	545	135
Grayland Plains	335	1070	735	560	520	175
Long Beach	285	1150	865	660	620	245
Clatsop Plains	260	1195	935	570	540	215

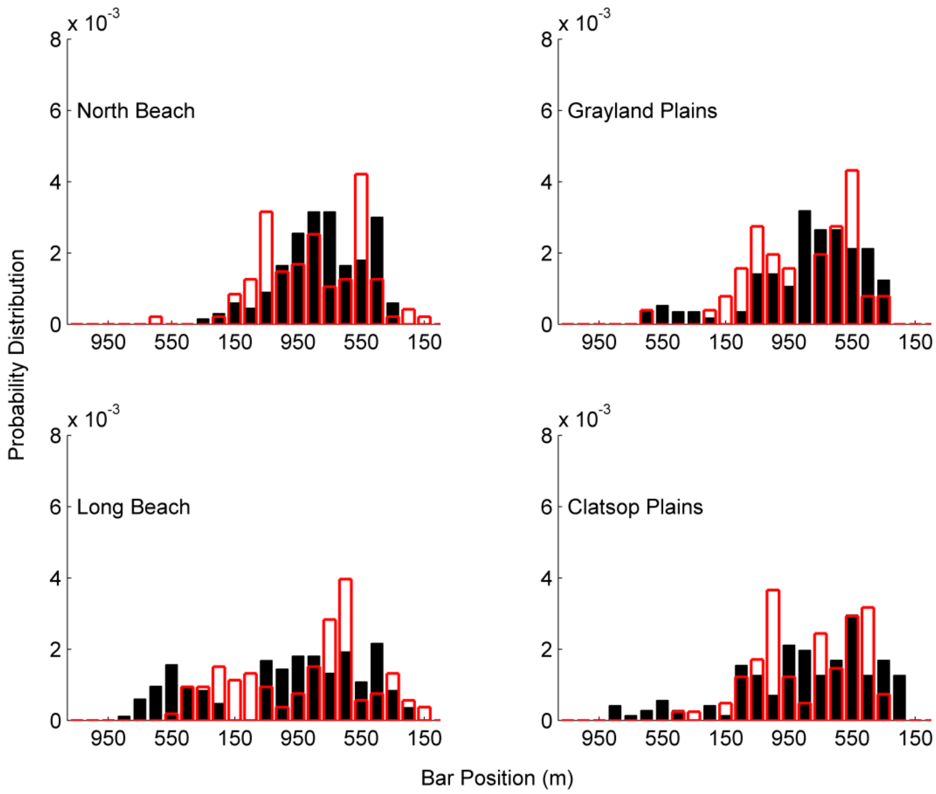

Figure 22. Probability distribution functions of bar position for the CRLC littoral cells. Black bars represent the temporal data. Red outlined bars represent the spatial data. Bin widths are 50m.

Table 11. Temporal Bar Depth Statistics

Littoral Cell	Maximum bar depth (m)	Minimum bar depth (m)	Depth range of bar zone (m)	Mean bar depth (m)	Median bar depth (m)	Std (m)
North Beach	4.9	1.5	3.4	3.0	2.9	0.9
Grayland Plains	6.7	1.6	5.1	3.4	3.3	1.3
Long Beach	6.8	1.6	5.2	3.9	3.5	1.5
Clatsop Plains	8.2	1.5	6.7	3.8	3.3	1.7

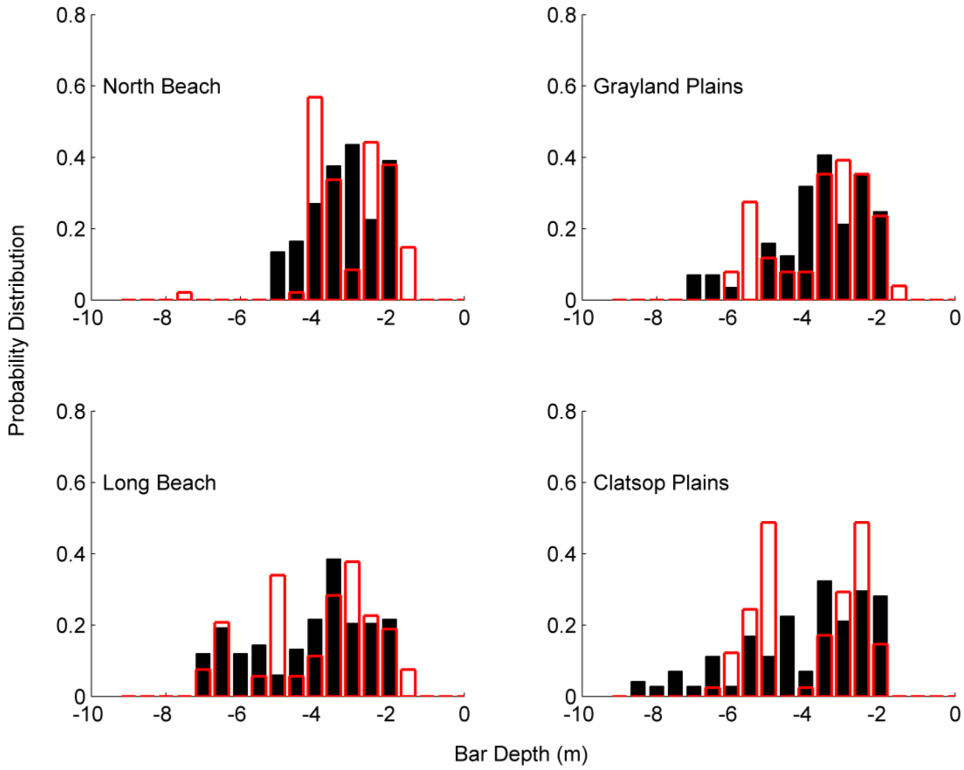

Figure 23. Probability distribution functions of bar depth for each of the CRLC littoral cells. Black bars represent the temporal data. Red outlined bars represent the spatial data. Bin widths are 0.5m.

Table 12. Temporal Bar Height Statistics. Mean bar heights in parentheses represent the mean without the zero heights associated with nearshore terraces.

Littoral Cell	Maximum bar height (m)	Mean bar height (m)	Median bar height (m)	Std (m)
North Beach	1.8	0.4 (0.7)	0.3	0.4
Grayland Plains	1.9	0.4 (0.8)	0.3	0.5
Long Beach	4.4	0.9 (1.3)	0.7	1.0
Clatsop Plains	3.8	0.7 (1.2)	0.8	0.9

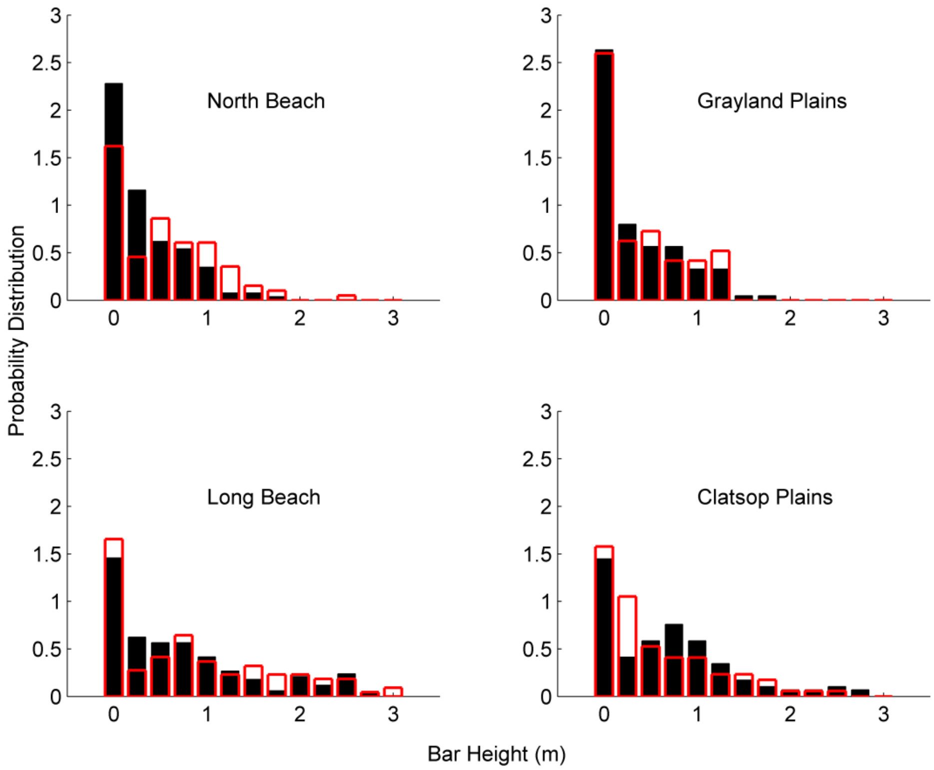

Figure 24. Probability distribution functions of bar height for each of the CRLC littoral cells. Black bars represent the temporal data. Red outlined bars represent the spatial data. Bin widths are 0.25m.

Table 13. T-Test for spatial and temporal variability compares the mean of a littoral cell in the spatial data (X) to the mean of the same littoral cell in the temporal data (Y). = indicates that the means are equal; < denotes that the mean of X is less than the mean of Y; > indicates that the mean of X is greater than the mean of Y. Littoral cell abbreviations are the same as in Table 3.

	Bar Position	Bar Depth	Bar Height
North Beach	=	=	>
Grayland Plains	=	=	=
Long Beach	<	=	=
Clatsop Plains	=	=	<

Table 14. Single bar system versus multiple bar system comparison over the entire time period of the data set. This ratio compares the number of years where the majority of profiles has only 1 bar to the number of years where the majority of profiles has 2 or more bars.

Littoral Cell	Single bar:multiple bars per profile (number of years)
North Beach	7:8
Grayland Plains	7:6
Long Beach	4:11
Clatsop Plains	4:9

5.3 Nearshore Terraces

Nearshore terraces make up nearly a third of the bars extracted from this data set. Descriptions of nearshore terrace features in the sandbar literature are rare. Pape et al. (2010) described a nearshore terrace as a bar that was not clearly separated from the shoreline by a trough and was observed to develop crescentic features. While some PNW terraces may be features not clearly separated from the shoreline, they are not found exclusively near the shoreline. PNW terraces can be found at every depth where bars are found, and vary in size and shape (Figure 25).

In some instances, we interpret the zero bar height of terraces to be related to spatial bar decay. Spatial bar decay is observed as the disappearance, in the longshore direction, of an otherwise longshore continuous bar. Walstra et al. (2012) and Ruessink et al. (2003) have also observed a relationship between decreasing bar height and the offshore bar decay component of NOM. Examples of terraces related to bar decay can be found in Figure 26, Figure 27, and Figure 28. In Long Beach the outer bar (Bar 1) that is visible in the southern section of Figure 26 decays offshore in space to the north of the littoral cell. Following the bar north from approximately 5131km N, the bar height decreases until at approximately 5146km N it is characterized as a terrace (denoted by the transition from a circle symbol to a triangle symbol). Further north, at approximately 5147km N, the bar decays completely and is not longer found in subsequent profiles. Spatial bar decay can also be seen in Grayland in the outer bar denoted as Bar 1 (Figure 27; Figure 28). Following the bar to the north once more, we see bar height decay to zero, and then the feature disappears. Figure 28 shows these changes in profile view; the bar that is clearly visible in transect 36 becomes a terrace in transect 43 and is not visible in transect 47.

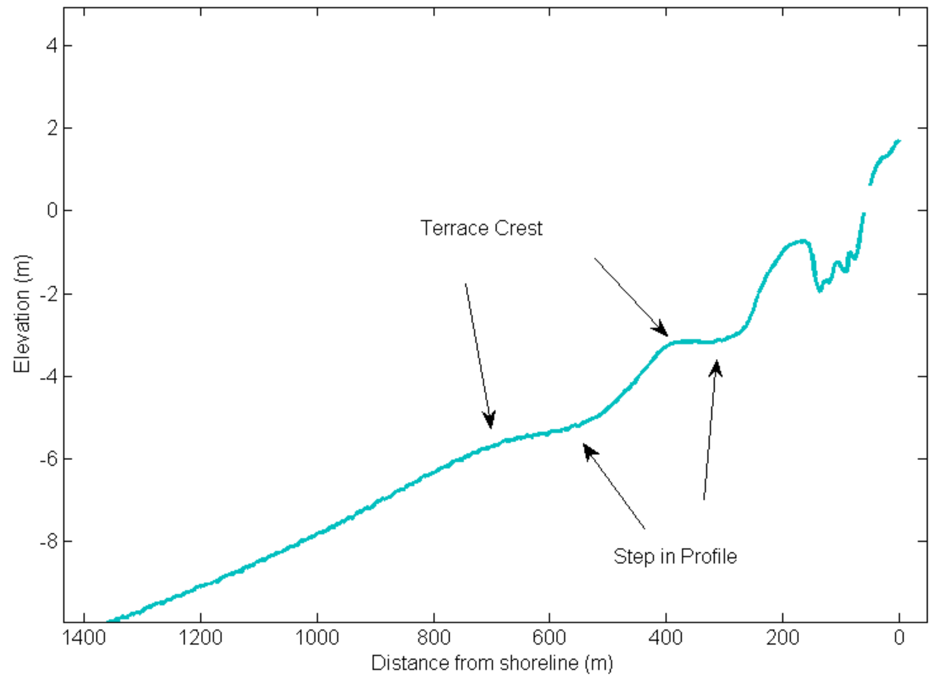

Figure 25. Terrace morphology definition sketch. Transect 85 from Grayland Plains.

a.

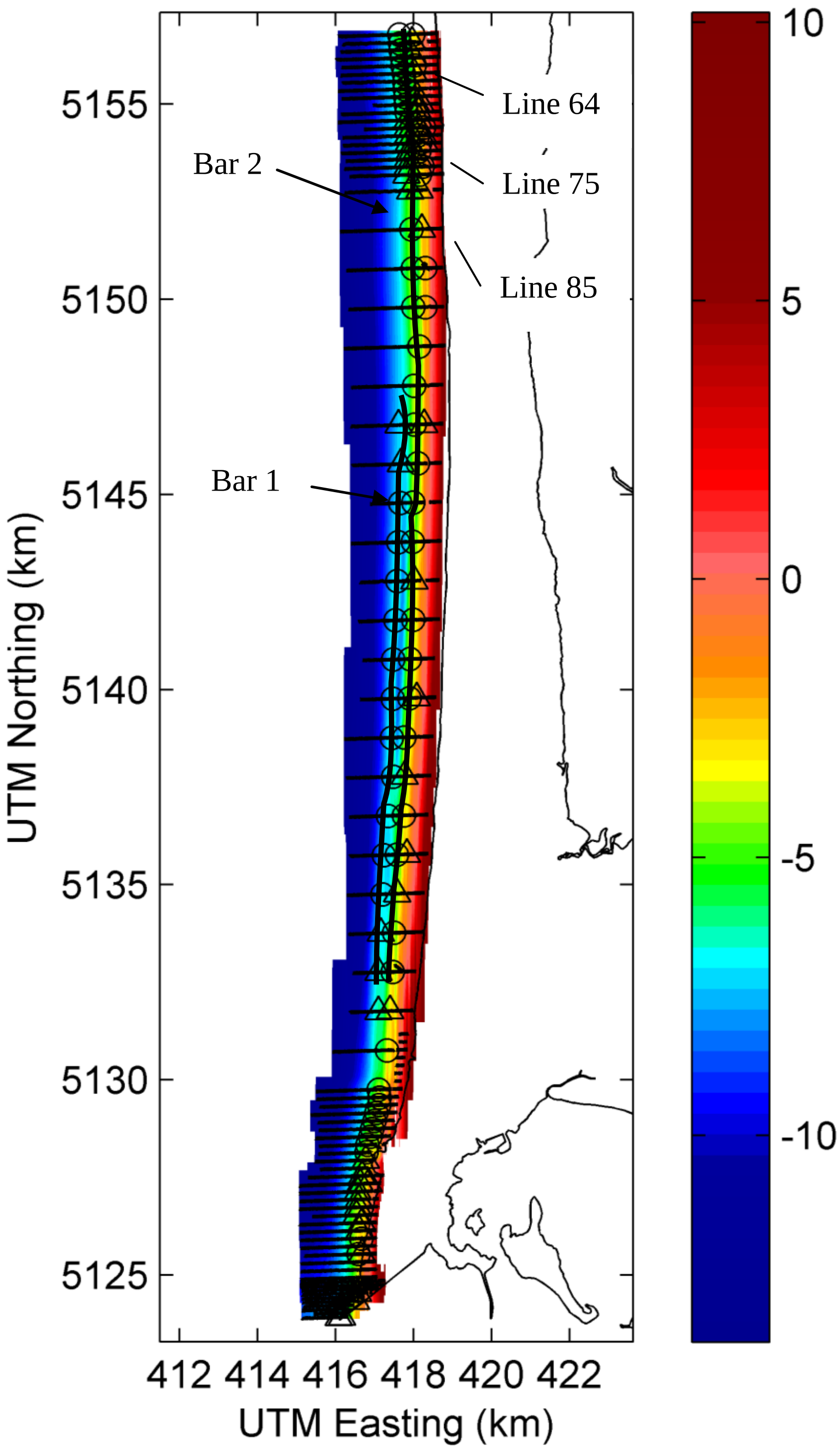
Line 64
Line 75
Line 85
Bar 2
Bar 1
5155
5150
5145
5140
5135
5130
5125
UTM Northing (km)
412 414 416 418 420 422
UTM Easting (km)
10
5
0
-5
-10

b.

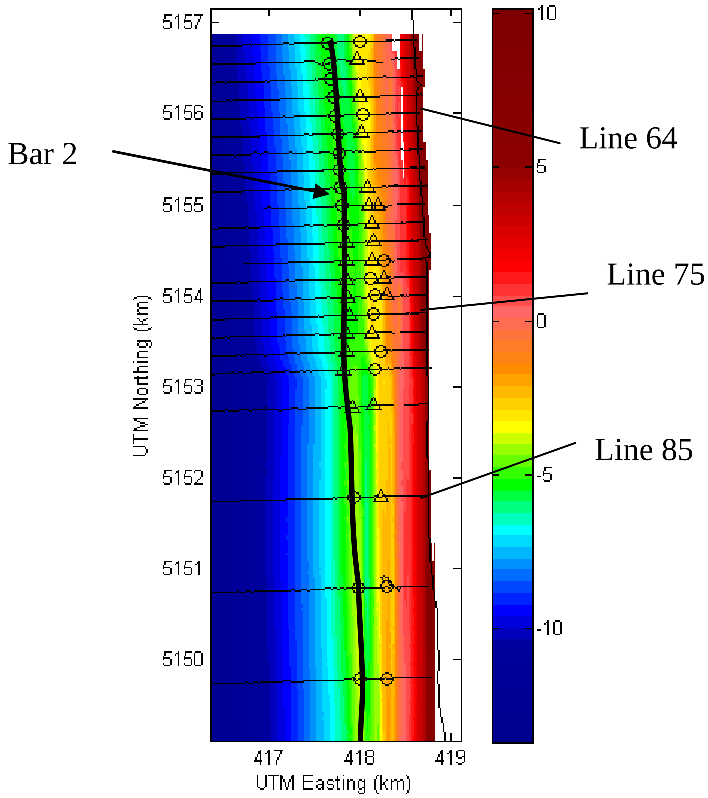

Figure 26. An interpolated surface of Long Beach (2011) shows longshore continuous bars. Extracted bars with significant heights are marked with a circle. Terraces are marked with a triangle. The colorbar represents depth in meters. Panel a. shows the entirety of the littoral cell. Panel b. shows an enlarged view of the northern area of the littoral cell.

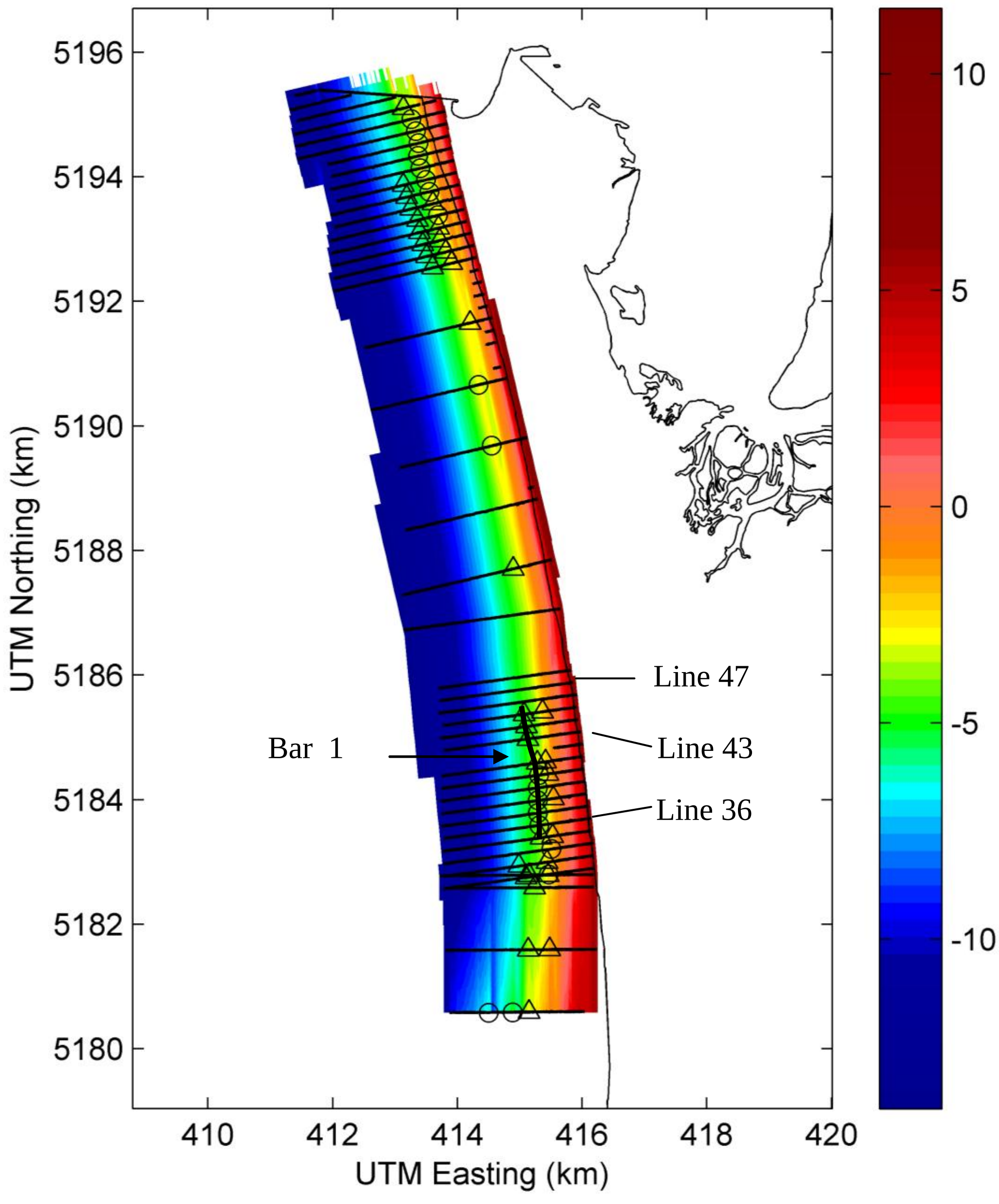

Figure 27. An interpolated surface of Grayland Plains (2011) shows longshore continuous bars. Extracted bars with significant heights are marked with a circle. Terraces are marked with a triangle. Color bar represents depth in meters.

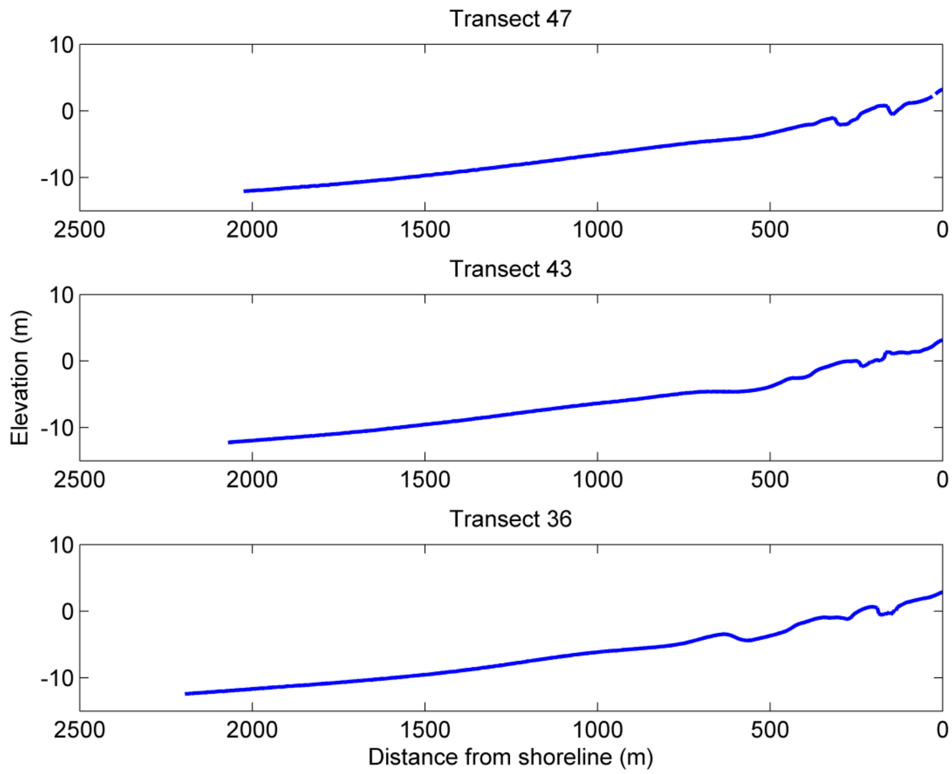

Figure 28. Grayland Plains (Bar 1) terraces in profile view showing bar decay. The outer terrace gradually disappears to the north (Transect 36 through Transect 47). The spatial distribution of profiles is labeled on Figure 27.

In other instances the relationship between terraces and bar decay is not evident. A longshore continuous bar can be both a bar, with non-zero height, and a terrace, with zero height, at the same time, but in different locations (Figure 26; Figure 29). Consider the bar in Long Beach that is the middle bar at the southern end of the littoral cell and the outer bar at the northern end, denoted Bar 2 (Figure 26). This feature begins as a bar with non-zero height, but becomes a terrace near 5152km N (Figure 26b). Further north, near 5154km N, the bar again has non-zero height. The changing morphology can be seen in profile view in Figure 29. The bar clearly decreases in height until it is a step in the profile and then increases in height to become a bar again. The height range for this bar is 0m to 2.9m over 25km of observations. The bar is observed to be longshore continuous over this distance. This bar is simultaneously one of the tallest bars and one of the shortest bars in Long Beach, depending on where it is sampled. Clearly, the causes of terrace morphology are more complex than simply bar decay alone.

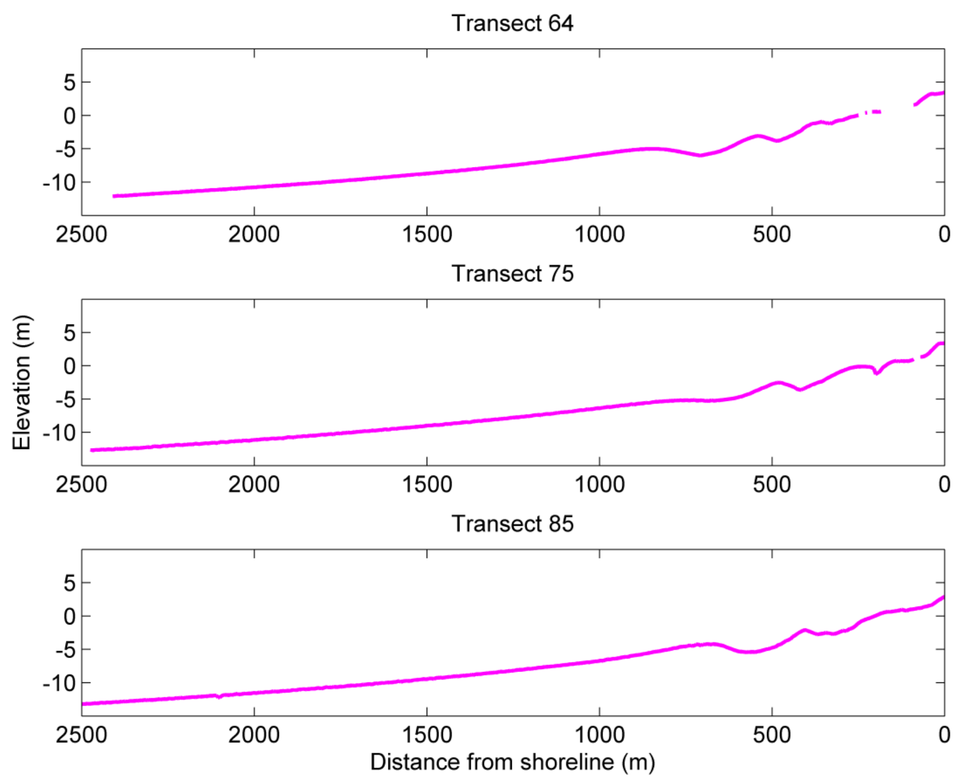

Figure 29. Long Beach terraces (Bar 2) in profile view show variable bar height in space. Spatial position of these profile can be seen in Figure 26.

6 Conclusions

We have used a regional scale data set of nearshore bathymetry to describe and quantify the variability of sandbar morphology and explore environmental variables that influence the observed bar variability. From north to south along an approximately 250km stretch of Pacific Northwest coast: the width of the effective bar zone decreases, the mean bar position decreases, and the maximum bar position decreases. Higher upper shoreface slopes are also associated with a transition from transects with predominantly multiple bars per profile to transects with a single bar per profile. Sandbar depths are much more spatially consistent, and the mean depths for most of the littoral cells examined are not statistically different from each other. Of the environmental variables investigated here, the most substantial regional scale trend observed was the north to south steepening trend in upper shoreface slope. Correlation analyses between environmental variables and bar morphometrics show significant correlations between slope and bar position and also between breaking wave height and depth range and breaking wave length and depth range. Steepening of the upper shoreface slope is associated with decreasing bar positions from the shoreline. Higher breaking wave height and breaking wave length are connected with greater depth ranges. No significant correlations between bar morphometrics and tide range, grain size, wave direction, wavelength, or dimensionless fall velocity were found.

7 References

Allan, J.C., and Komar, P.D., 2002, Extreme Storms on the Pacific Northwest Coast during the 1997-98 El NiNo and the 1998-99 La Nina: Journal of Coastal Research, v. 18, no. 1, p. 175–193.

Beach, R.A., Holman, R.A., and Stanley, J., 1994, Measuring nearshore bathymetry on high energy beaches: American Geophysical Union Fall Meeting, San Francisco.,.

Birkemeier, W.A., 1984, Time Scales of Nearshore Porfile Changes: Proceedings of the International Conference on Coastal Engineering, v. 1, no. 19.

Clemens, K.E., and Komar, P.D., 1988, Oregon Beach-sand Compositions Produced by the Mixing of Sediments Under a Transgressing Sea: Journal of Sedimentary Petrology, v. 58, no. 3, p. 519–529.

Daniels, R.C., Ruggiero, P., and Weber, L.E., 1999, Washington coastal geodetic control network: report and station index.: Washington Department of Ecology Publication, v. 99, no. 103, p. 268.

Van Enckevort, I.M.., and Ruessink, B.G., 2003a, Video observations of nearshore bar behaviour. Part 1: alongshore uniform variability: Continental Shelf Research, v. 23, no. 5, p. 501–512, doi: 10.1016/S0278-4343(02)00234-0.

Van Enckevort, I.M.., and Ruessink, B.G., 2003b, Video observations of nearshore bar behaviour. Part 2: alongshore non-uniform variability: Continental Shelf Research, v. 23, no. 5, p. 513–532, doi: 10.1016/S0278-4343(02)00235-2.

Garcia-Medina, G., Ozkan-Haller, T., and Ruggiero, P., 2012, Nearshore Wave Predictions along the Oregon and Southwest Washington Coast: Oregon State University.

García-Medina, G., Özkan-Haller, H.T., Ruggiero, P., and Oskamp., J. An Inner-Shelf Wave Forecasting System for the US Pacific Northwest: Weather and Forecasting,.

Gelfenbaum, G., and Kaminsky, G.M., 2010, Large-scale coastal change in the Columbia River littoral cell: An overview: Marine Geology, v. 273, no. 1-4, p. 1–10, doi: 10.1016/j.margeo.2010.02.007.

Grunnet, N.M., and Hoekstra, P., 2004, Alongshore variability of the multiple barred coast of Terschelling, The Netherlands: Marine Geology, v. 203, no. 1-2, p. 23–41, doi: 10.1016/S0025-3227(03)00336-0.

Kaminsky, G.M., Ruggiero, P., Buijsman, M.C., McCandless, D., and Gelfenbaum, G., 2010, Historical evolution of the Columbia River littoral cell: Marine Geology, v. 273, no. 1-4, p. 96–126, doi: 10.1016/j.margeo.2010.02.006.

Komar, P.D., 1998, The Pacific Northwest Coast: Living with the shores of Oregon and Washington: Duke University Press.

Komar, P.D., and Gaughan, M.K., 1976, Airy Wave Theory and Breaker Height Prediction: Coastal Engineering, , no. 4.

Kuriyama, Y., 2012, Process-based one-dimensional model for cyclic longshore bar evolution: Coastal Engineering, v. 62, p. 48–61, doi: 10.1016/j.coastaleng.2011.12.001.

Lippmann, T.C., and Holman, R.A., 1990, The Spatial and Temporal Variability of Sand Bar Morphology: Journal of Geophysical Research, v. 95, no. C7, p. 11,575–11,590.

Lippmann, T.C., Holman, R.A., and Hathaway, K.K., 1993, Episodic, Nonstationary Behavior of a Double Bar System at Duck, North Carolina, U.S.A., 1986–1991: Journal of Coastal Research, v. SI, no. 15, p. 49–75.

List, J.H., and Terwindt, J.H.J., 1995, Large-scale coastal behavior: Marine Geology, v. 126, no. 1-4, p. 1–3, doi: 10.1016/0025-3227(95)00062-4.

MacMahan, J.H., 2001, HYDROGRAPHIC SURVEYING FROM PERSONAL WATERCRAFT: Journal of Surveying Engineering, v. 127, p. 12–24.

Masselink, G., and Hughes, M., 2003, An Introduction to Coastal Processes and Geomorphology: Hodder Education, London.

Masselink, G., and Short, A.D., 1993, The Effect of Tide Range on Beach Morphodynamics Morphology : A Conceptual Beach Model: , no. 1984.

Pape, L., Kuriyama, Y., and Ruessink, B.G., 2010, Models and scales for cross-shore sandbar migration: Journal of Geophysical Research, v. 115, no. F3, doi: 10.1029/2009JF001644.

Peterson, C.D., Darienzo, M.E., Hamilton, D., Pettit, D.J., and Yeager, R.K., 1994, Cascadia Beach-Shoreline Data Base, Pacific Northwest Region, USA: Open File Report 0-94-2, v. 03, no. 2, p. 1–26.

Peterson, C.D., Jol, H.M., Vanderburgh, S., Phipps, J.B., Percy, D., and Gelfenbaum, G., 2010a, Dating of late Holocene beach shoreline positions by regional correlation of coseismic retreat events in the Columbia River littoral cell, USA: Marine Geology, v. 273, no. 1-4, p. 44–61, doi: 10.1016/j.margeo.2010.02.003.

Peterson, C.D., Vanderburgh, S., Roberts, M.C., Jol, H.M., Phipps, J., and Twichell, D.C., 2010b, Composition, age, and depositional rates of shoreface deposits under barriers and beach plains of the Columbia River littoral cell, USA: Marine Geology, v. 273, no. 1-4, p. 62–82, doi: 10.1016/j.margeo.2010.02.004.

Plant, N.G., Holland, K.T., and Puleo, J.A., 2002, Analysis of the scale of errors in nearshore bathymetric data: Marine, v. 191, p. 71–86.

Plant, N.G., Holman, R.A., and Freilich, M.H., 1999, A simple model for interannual sandbar behavior: Journal of Geophysical Research, v. 104, no. C7.

Ruessink, B.G., and Kroon, A., 1994, The behaviour of a multiple bar system in the nearshore zone of Terschelling, the Netherlands; 1965-1993: Marine Geology, v. 121, no. 3-4, p. 187–197.

Ruessink, B.G., Kuriyama, Y., Reniers, A.J.H.M., Roelvink, J.A., and Walstra, D.J.R., 2007, Modeling cross-shore sandbar behavior on the timescale of weeks: Journal of Geophysical Research, v. 112, no. F3, p. @F03010.

Ruessink, B.G., and Terwindt, J.H.J., 2000, The behaviour of nearshore bars on the time scale of years: a conceptual model: Marine Geology, v. 163, no. 1-4, p. 289–302, doi: 10.1016/S0025-3227(99)00094-8.

Ruessink, B.G., Wijnberg, K.M., Holman, R.A., Kuriyama, Y., and Van Enckevort, I.M.., 2003, Intersite comparison of interannual nearshore bar behavior: Journal of Geophysical Research, v. 108, no. C8, doi: 10.1029/2002JC001505.

Ruggiero, P., Eshleman, J.L., Kingsley, E., Thompson, D.M., Voigt, B., Kaminsky, G.M., and Gelfenbaum, G., 2007, Beach Morphology Monitoring in the Columbia River Littoral Cell : 1997 – 2005: Report: U.S. Geological Survey Data Series 260,, p. 1997–2005.

Ruggiero, P., Kaminsky, G.M., Gelfenbaum, G., and Voigt, B., 2005, Seasonal to Interannual Morphodynamics along a High-Energy Dissipative Littoral Cell: Journal of Coastal Research, v. 213, p. 553–578, doi: 10.2112/03-0029.1.

Ruggiero, P., Komar, P.D., Mcdougal, W.G., Marra, J.J., Reggie, A., and Spring, F., 2001, Wave Runp, Extreme Water Levels and the Erosion of Properties Properties Backing Beaches: Journal of Coastal Research, v. 17, no. 2, p. 407–419.

Ruggiero, P., Kratzmann, M.G., Himmelstoss, E.A., Reid, D., Allan, J.C., and Kaminsky, G.M., 2012, National Assessment of Shoreline Change : Historical Shoreline Change along the Pacific Northwest coast: U.S. Geological Survey: Open File Report, v. 2012-1007.

Ruggiero, P., and Voigt, B., 2000, Beach Monitoring in the Columbia River Littoral Cell , 1997-2000: Department of Ecology Publication, , no. 00-06-26.

Sallenger, A.H., Krabill, W.B., Swift, R.N., Brock, J., List, J., Hansen, M., Holman, R.A., Manizade, S., Sontag, J., Meredith, A., Morgan, K., Yunkel, J.K., Frederick, E.B., and Stockdon, H., 2003, Evaluation of airborne topographic lidar for quantifying beach changes.: Journal of Coastal Research, v. 19, no. 1, p. 125–133.

Smith, E.R., Wang, P., Ebersole, B. a., and Zhang, J., 2009, Dependence of Total Longshore Sediment Transport Rates on Incident Wave Parameters and Breaker Type: Journal of Coastal Research, v. 253, no. 2002, p. 675–683, doi: 10.2112/07-0919.1.

Vanderburgh, S., Roberts, M.C., Peterson, C.D., Phipps, J.B., and Herb, A., 2010, Transgressive and regressive deposits forming the barriers and beachplains of the Columbia River Littoral Cell, USA: Marine Geology, v. 273, no. 1-4, p. 32–43, doi: 10.1016/j.margeo.2010.02.002.

Walstra, D.J.R., Reniers, a. J.H.M., Ranasinghe, R., Roelvink, J.A., and Ruessink, B.G., 2012, On bar growth and decay during interannual net offshore migration: Coastal Engineering, v. 60, p. 190–200, doi: 10.1016/j.coastaleng.2011.10.002.

Weber, K.M., List, J.H., and Morgan, K.L.M., 2005, An Operational Mean High Water Datum for Determination of Shoreline Position from Topographic Lidar Data: Open File Report, , no. 2005-1027.

Wijnberg, K.M., 2002, Environmental controls on decadal morphologic behavior of the Holland coast: Marine Geology, v. 189, no. 02, p. 227–247.

Wijnberg, K.M., and Terwindt, J.H.J., 1995, Extracting decadal morphological behaviour from high-resolution, long-term bathymetric surveys along the Holland coast using eigenfunction analysis: Marine Geology, v. 126, no. 1-4, p. 301–330, doi: 10.1016/0025-3227(95)00084-C.

Wright, L.., and Short, A.D., 1984, Morphodynamic variability of surf zones and beaches: A synthesis: Marine Geology, v. 56, no. 1-4, p. 93–118, doi: 10.1016/0025-3227(84)90008-2.